Substrate and Stereochemical Control of Peptidoglycan Cross-Linking by Transpeptidation by Escherichia coli PBP1B

Catherwood, Anita C.; Lloyd, Adrian J.; Tod, Julie A.; Chauhan, Smita; Slade, Susan E.; Walkowiak, Grzegorz P.

Published in:
Journal of the American Chemical Society

DOI:
10.1021/jacs.9b08822

Publication date:
2020

Document Version
Peer reviewed version

Article

Substrate and stereochemical control of peptidoglycan crosslinking by transpeptidation by Escherichia coli PBP1B

Anita C. Catherwood, Adrian J. Lloyd, Julie A. Tod, Smita Chauhan, Susan E. Slade, Gregory Walkowiak, Nicola F. Galley, Avinash Punekar, Katie Smart, Dean Rea, Neil D Evans, Michael J Chappell, David I. Roper, and Christopher G Dowson

J. Am. Chem. Soc., **Just Accepted Manuscript** • DOI: 10.1021/jacs.9b08822 • Publication Date (Web): 12 Feb 2020

Substrate and stereochemical control of peptidoglycan cross-linking by transpeptidation by *Escherichia coli* PBP1B

Anita C. Catherwood[$], Adrian J. Lloyd[+$], Julie A. Tod, Smita Chauhan[@], Susan E. Slade[†], Grzegorz P. Walkowiak [‡], Nicola F. Galley[¶], Avinash S. Punekar[§], Katie Smart, Dean Rea[#], Neil D. Evans[*], Michael J. Chappell[*], David I. Roper and Christopher G. Dowson[+] School of Life Sciences, University of Warwick, Gibbet Hill Road, Coventry, CV4 7AL, UNITED KINGDOM.

ABSTRACT: Penicillin binding proteins (PBPs) catalysing transpeptidation reactions that stabilize the peptidoglycan component of the bacterial cell wall are the targets of β-lactams, the most clinically successful antibiotics to date. However, PBP-transpeptidation enzymology has evaded detailed analysis, because of the historical unavailability of kinetically competent assays with physiologically relevant substrates and the previously unappreciated contribution of protein cofactors to PBP activity. By re-engineering peptidoglycan synthesis, we have constructed a continuous spectrophotometric assay for transpeptidation of native or near native peptidoglycan precursors and fragments by *Escherichia coli* PBP1B, allowing us to (a) identify recognition elements of transpeptidase substrates, (b), reveal a novel mechanism of stereochemical editing within peptidoglycan transpeptidation, (c) assess the impact of peptidoglycan substrates on β-lactam targeting of transpeptidation and (d) demonstrate both substrates have to be bound before transpeptidation occurs. The results allow characterization of high molecular weight PBPs as enzymes and not merely the targets of β-lactam acylation.

INTRODUCTION

Peptidoglycan is a polymer of alternating N-acetyl glucosaminyl (GlcNAc) and N-acetyl muramyl (MurNAc) saccharides appended to which are penta, tetra or tripeptides, crosslinked to impart mechanical rigidity essential for bacterial viability[1]. The transpeptidases responsible for these crosslinks, the PBPs, are targets of β-lactams which were discovered ninety years ago[2], and comprise the most clinically valuable antimicrobials[3,4]. β-lactam resistance, due to extended spectrum β-lactamases has contributed to infections resistant to virtually all clinical antibiotics[5], highlighting the necessity for new PBP transpeptidation inhibitors.

PBPs possess an active site serine acylated by the donor peptidoglycan pentapeptide, with release of its C-terminal *D*-alanine. This acyl-enzyme reacts with water or an amine of a second peptidoglycan peptide, termed an acceptor, constituting *D,D*-carboxypeptidation or transpeptidation reactions respectively[6-9]. Transpeptidase PBPs are mono-functional (Type B) or contain additional catalytic sites (Type A) that polymerise by transglycosylation a peptidoglycan lipid-linked precursor[6,7]. In *E. coli* this is undecaprenyl pyrophosphoryl GlcNAc-MurNAc *L*-alanyl-γ-*D*-glutamyl-*meso*-diaminopimelyl-*D*-alanyl-*D*-alanine, (lipid II-*meso*-DAP[9]; DAP denotes diaminopimelic acid). An impediment to novel targeting of PBPs was the inability to define their biochemistry beyond their acylation by β-lactams[10] which has been pursued without substrates, an omission inconsistent with the competition with peptidoglycan precursors that β-lactams have to overcome *in vivo*. PBP substrates have until recently[11,12] remained unattainable and are key to understanding and translational exploitation of β-lactam:PBP interactions.

E. coli possesses three bifunctional type A PBPs, 1A, 1B and 1C[7]. Without PBP1A or PBP1B, PBP1B or PBP1A respectively, are essential[13-15]. *E. coli* PBP1B is localised and activated by the outer membrane protein LpoB[16-18]. Critically, however, lack of quantitative transpeptidase assays with physiological substrates has severely limited analysis of PBP1B transpeptidation and translational progress towards its exploitation as an antibiotic target.

Here, we describe an LCMSMS-validated continuous photometric transpeptidase assay for *E. coli* PBP1B, which we use to quantitate the impact of LpoB on PBP1B and probe transpeptidase substrate structure-activity relationships, revealing how stereochemical fidelity of transpeptidation is maintained. We characterise the impact of peptidoglycan substrates on β-lactam-inhibition of PBP1B suggesting acceptor and donor binding prior to transpeptidation, which we confirm by steady state kinetics. Therefore, following the ninetieth anniversary of the discovery of penicillin[2], we give the most detailed enzymatic account thus far of peptidoglycan transpeptidation that is targeted by this most clinically essential class of antibiotics.

RESULTS

Development of a continuous assay for PBP transpeptidation. To analyse *E. coli* PBP1B transpeptidation kinetics, a continuous assay for this activity was devised: *D*-alanine generated by PBP1B was oxidised by *D*-amino acid oxidase yielding hydrogen peroxide which was detected by horseradish peroxidase-catalysed conversion of amplex red to the chromophore resorufin (Scheme 1).

Initial attempts to follow transpeptidation required prohibitive (> 1 μM) amounts of PBP1B. However, addition of LpoB, allowed measurement of lipid II-*meso*-DAP and PBP1B-dependent rates with < 10 nM PBP1B (Figure 1a), where utilising lipid II-Lys and MurNAc *L*-alanyl-γ-*D*-glutamyl-*meso*-DAP-*D*-alanyl-*D*-alanine (MurNAc *meso*-DAP pentapeptide), dependence of PBP1B activity on LpoB was hyperbolic with a half maximal activation at 0.26 ± 0.02 μM LpoB, and a maximal stimulation of PBP1B of 1140 ± 20 fold (Figure 1b). PBP1B activity with lipid II-*meso*-DAP was also essentially dependent on LpoB, which activated the enzyme >250-fold (Figure 1 bi). Therefore 1.97 μM LpoB was included in all assays from hereon. The assay was linearly dependent on *E. coli* PBP1B, utilising lipid II-*meso*-DAP or lipid II-Lys with MurNAc *meso*-DAP pentapeptide (Figure 1c).

We used LCMS and LCMSMS of mutanolysin-digested PBP1B products (**S.1.2.3.2.1.)** to determine if PBP1B-catalysed *D*-alanine release from lipid II-*meso*-DAP reported transpeptidation, and detected products with m/z values of GlcNAc-MurNAc *L*-alanyl-γ-*D*-glutamyl-*meso*-DAP-*D*-alanyl donor bonded *via* the carbonyl of its C-terminal *D*-alanyl residue to the ε-amine of the *meso*-DAP of the GlcNAc-MurNAc *L*-alanyl-γ-*D*-glutamyl-*meso*-DAP-*D*-alanyl-*D*-alanine acceptor (Figure 2a). The molecule fractionated into three anomers (Figure 2c; expected $(m+2H^+)/2$ = 966.92, found = 966.91, 966.92 and 966.92). LCMSMS of ions eluting at 7.92 minutes (Figure 2d, Table S3) confirmed the 966.92 ion was the PBP1B transpeptidation product. Identical fragmentation of 966.92 ions eluting at 7.65 and 7.31 minutes was also observed. Higher order products with three or four disaccharide peptides linked by transpeptidation (expected $m+2H^+)/2$ = 1427.10 and 1887.79 were not detected, even if the concentration of PBP1B in the LCMS assays was increased 100-fold to 1 μM.

D-alanine release could additionally have originated from PBP1B-*D,D*-carboxypeptidation. LCMS detected the *D,D*-carboxypeptidase-generated tetrapeptide GlcNAc-MurNAc *L*-alanyl-γ-*D*-glutamyl-*meso*-DAP-*D*-alanine (Figure 2b) as two anomer peaks at ~1% of the abundance of the transpeptidation product (Figure 2c), (observed and expected $m+H^+)/1$ both peaks = 940.40; Figure S3aii). LCMSMS confirmed both peaks were GlcNAc-MurNAc tetrapeptide (Figure S3ai; Table S4), suggesting *D*-alanine release from lipid II-*meso*-DAP overwhelmingly followed transpeptidation relative to carboxypeptidation.

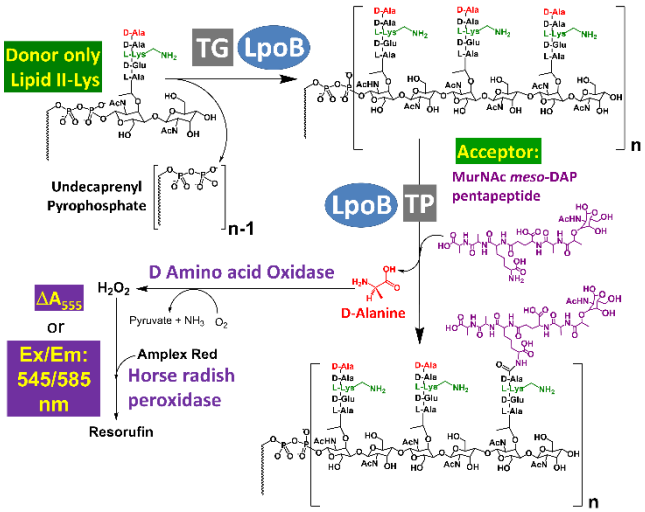

Scheme 1: Continuous photometric assay of PBP1B transpeptidation. The scheme shows the detection of D-alanine generated in a format where the substrates act exclusively as donor or acceptor. TG = transglycosylase, TP = transpeptidase.

Refinement of the PBP1B transpeptidation continuous assay to distinguish between donor and acceptor utilization. In *E. coli* peptidoglycan synthesis, lipid II-*meso*-DAP serves both as acceptor and donor. Therefore, to study PBP1B transpeptidase substrate utilization required exclusive donors and acceptors. As lipid II-Lys is only a donor[19,20] we challenged PBP1B with lipid II-Lys which supported low rates of *D*-alanine release. Striking enhancements of *D*-alanine release occurred (≥10-fold) when MurNAc *meso*-DAP pentapeptide as acceptor was added (Figure 1d,e).

We confirmed the assay followed PBP1B activity showing that ampicillin inhibited transpeptidation (Figure 1e). The drug at 50 μM was without impact on *D*-amino acid oxidase or horse radish peroxidase activity. Only at 11.5 mM or 14.3 mM ampicillin respectively, was any reduction of oxidase and peroxidase activity observed (18.2% and 26% inhibition respectively). Therefore, the impact of the concentrations of ampicillin used hence forth on the coupling enzymes could be ignored.

To establish the coupling system reported PBP1B transpeptidation we omitted *D*-amino acid oxidase from the assay. Its subsequent re-addition caused an instantaneous increase in absorbance, to that had the oxidase always been present (Figure 1f), suggesting the assay measured PBP1B transpeptidation, un-influenced by consumption of the *D*-alanine. (Figure 1f).

We confirmed enhancement of PBP1B-catalysed *D*-alanine release from Lipid II-Lys by MurNAc *meso*-DAP pentapeptide followed transpeptidation by LCMS and LCMSMS: We detected the transpeptidation product GlcNAc-MurNAc *L*-alanyl-γ-*D*-glutamyl-L-lysyl-*D*-alanyl donor stem bonded *via* the carbonyl of the C-terminal *D*-alanyl to the ε-amine of the *meso*-DAP of the MurNAc *meso*-DAP pentapeptide acceptor (Figure S4a,b; expected/observed $(m+2H^+)/2$ = 843.38/843.38) and confirmed its identity by LCMSMS. (Figure S4c; Table S5). Consistent with Figure 1e and[19,20] we could not detect lipid II-Lys donor/lipid

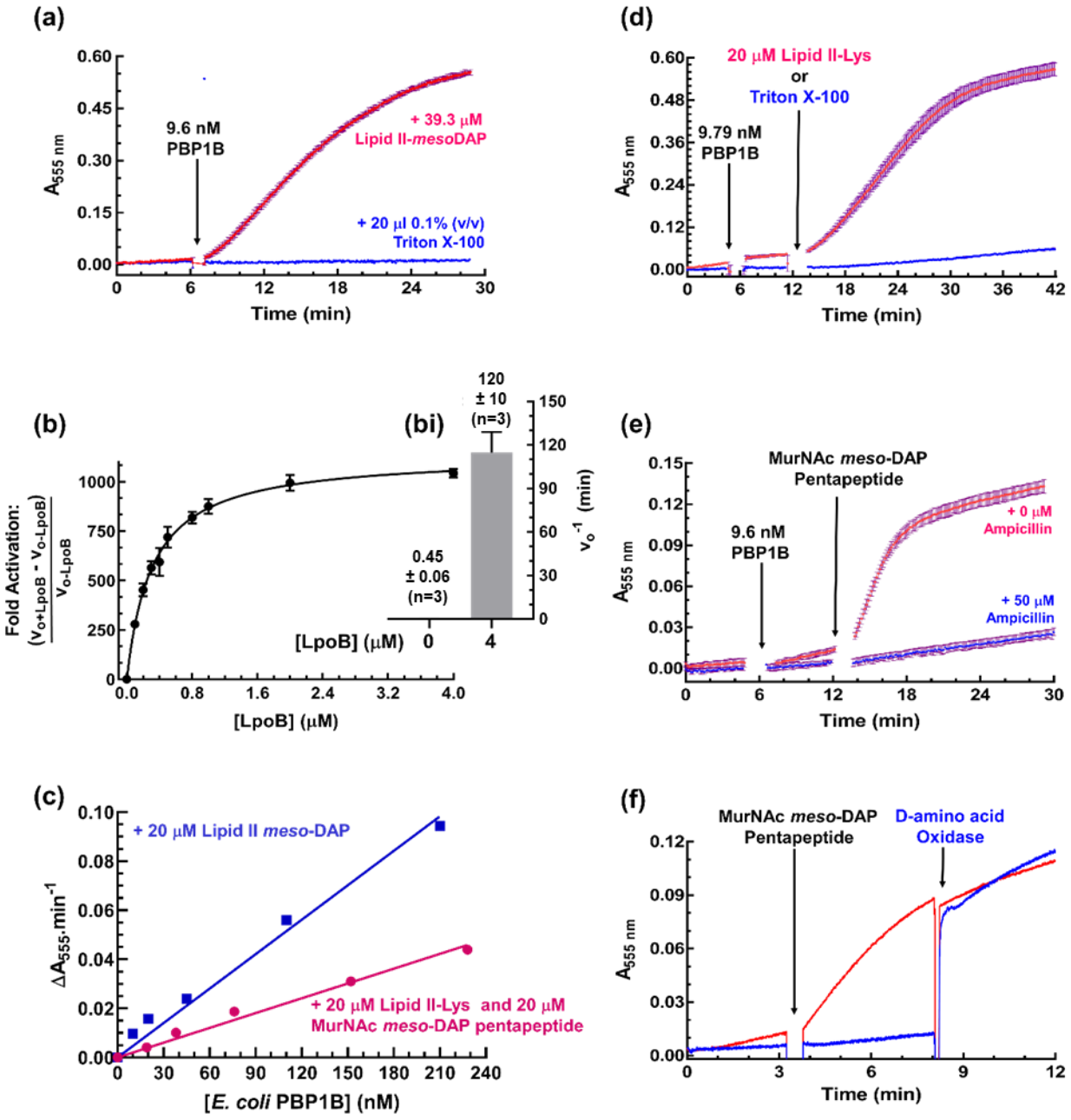

Figure 1: Characterization of *E. coli* PBP1B catalysis as reported by *D*-alanine release. **(a)** *D-alanine release by PBP1B from lipid II-meso-DAP*. Assay was performed with lipid II-*meso*-DAP or Triton X-100 and 1.97 μM LpoB. Data are mean ± standard deviation (S.D., n=3). **(b)** *Dependence of PBP1B D-alanine release on LpoB.* 11 nM *E. coli* PBP1B (except at 0 μM LpoB where [PBP1B] = 440 nM), were assayed with 20 μM lipid II-Lys or 20 μl 0.1% (v/v) Triton X-100 (control) and 20 μM MurNAc *meso*-DAP pentapeptide or **(bi)** with 20 μM lipid II-*meso*-DAP ± 4 μM LpoB. Data are mean ± S.D. (n=3). **(c)** *Dependence of PBP1B D-alanine release on PBP1B.* Assays containing 1.97 μM LpoB and 20 μM lipid II-*meso*-DAP or 20 μM lipid II-Lys with 20 μM MurNAc *meso*-DAP pentapeptide were initiated by PBP1B, controls replaced lipid II with 20 μl 0.1% (v/v) Triton X-100. **(d)** *D-alanine release by PBP1B from lipid II-Lys with a MurNAc meso-DAP pentapeptide acceptor*. Assay contained 80 μM MurNAc *meso*-DAP pentapeptide acceptor and 1.97 μM LpoB, with lipid II-Lys (red data points, maroon error bars) or Triton X-100 (blue data points, maroon error bars). The acceptor was added at zero time. All points are mean ± S.D. (n = 3). **(e)** *Inhibition of PBP1B transpeptidation by ampicillin.* Assays contained 20 μM lipid II-Lys, 20 μM MurNAc *meso*-DAP pentapeptide acceptor, 1.97 μM LpoB, *E. coli* PBP 1B, with (blue data points maroon error bars), or without (red data points, maroon error bars) 50 μM ampicillin. Ampicillin was added at zero time. Data are mean ± .SD. (n = 3). **(f)** *Lack of influence of D-alanine accumulation by PBP1B on the rate of transpeptidation.* Both assays contained 20 μM lipid II-Lys, 1.97 μM LpoB and 11 nM *E. coli* PBP 1B at zero time, however only one (red trace) contained *D*-amino acid oxidase. At 3.2 minutes, 20 μM MurNAc *meso*-DAP pentapeptide was added to both assays. At 8 minutes, 33.51 $U.ml^{-1}$ *Rhodotorula gracilis D*-amino acid oxidase was added to the assay from which it had been omitted at time zero (blue trace).

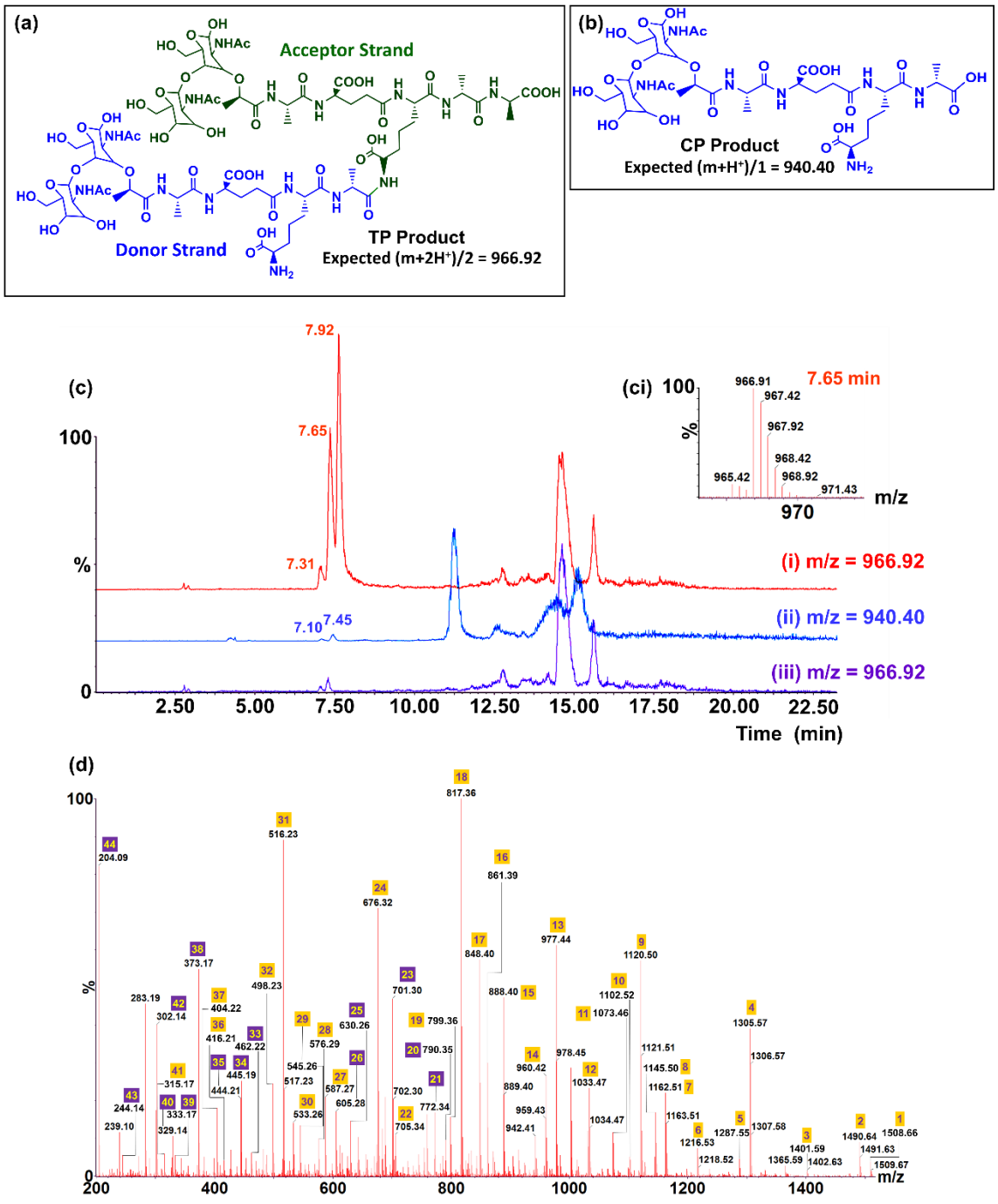

Figure 2: LCMS and LCMSMS analysis of *E. coli* PBP1B transpeptidation and carboxypeptidation products derived from lipid II-*meso*-DAP. (a) *Structure of transpeptidation product resulting from crosslinking of the stem peptides of lipid II-meso-DAP.* Green and blue peptides represent the acceptor and the donor strands respectively. Expected doubly charged m/z ratio is 966.92. **(b)** *Structure of carboxypeptidation product derived from the stem peptide of lipid II-meso-DAP.* Expected singly charged m/z ratio is 940.40. **(c)** *Extracted ion chromatograms of LCMS analysis of lipid II-meso-DAP transpeptidation.* Red and blue traces following the elution of species from a complete *E. coli* PBP1B assay with m/z ratios of 966.92 and 940.4. The purple trace is elution of 966.92 m/z species in assays omitting lipid II-*meso*-DAP. The 7.92, 7.65 and 7.31 minute peaks in the red trace and 7.45 and 7.1 minute peaks in the blue trace are likely anomers of the transpeptidation and carboxypeptidation products arising from muramidase digestion. The small doublet peak at 7.4 minutes in the purple trace may be due to carryover between samples or co-purification of *E.* coli PBP1B-bound peptidoglycan species. The inset **(ci)** are the ions of the doubly charged transpeptidation product. **(d)** *LCMSMS fragmentation of the 966.92 (m+2H⁺)/2 transpeptidation product eluting at 7.92 minutes.* All fragment ions were singly charged. All fragments containing acceptor and donor peptides linked by transpeptidation are labelled with purple numbers in yellow squares. All fragments originating exclusively from only donor or acceptor peptides are labelled with yellow numbers in purple squares. The identity of fragment ions 1 to 44 are displayed in Table S3.

II-Lys acceptor transpeptidation product by LCMS (expected $(m+H^+)/1$ = 1844.84; $(m+2H^+)/2$ = 922.92, neither found) confirming that lipid II-Lys could not act as an acceptor.

Without acceptor, PBP1B barely exhibited *D,D*-carboxypeptidase activity with lipid II-Lys spectrophotometrically. However this could be detected by LCMS and LCMSMS as GlcNAc-MurNAc *L*-alanyl-γ-*D*-glutamyl-*L*-lysyl-*D*-alanine tetrapeptide (Figure S5a-d). MurNAc *meso*-DAP pentapeptide ablated the tetrapeptide signal (Figure S5b) showing PBP1B minimised *D,D*-carboxypeptidase activity with a competent acceptor.

Lipid II transpeptidase donor polymerization triggers transpeptidase activity. PBP1B transpeptidation is predicated by transglycosylation[21-23]. To determine if lipid II polymerization or binding triggered transpeptidation we established a mass spectrometric assay for transglycosylation as release of undecaprenyl pyrophosphate (expected/observed (m-1)/1 of 925.62/ 925.62) from lipid II-Lys (Figure S6b) which was inhibited by 20 μM moenomycin as anticipated[21,22,24] (Figure S6a). Furthermore, moenomycin was a tight binding transpeptidation inhibitor (IC_{50} = 12.3 ± 0.9 nM; Figure S6c), confirming that transglycosylation predicated transpeptidase activity.

As moenomycin inhibition did not allow us to determine the importance of lipid II-Lys glycan chain polymerization to transpeptidation, we synthesised methylene lipid II-Lys (Figure S2, Tables S1 and S2) where the oxygen between the muramyl sugar C-1 and the β-phosphorus atom of the undecaprenyl pyrophosphoryl moiety was now a methylene (Figure S6d). This rendered methylene lipid II-Lys unpolymerisable because, instead of expulsion of undecaprenyl pyrophosphate on transglycosylation as is the case with lipid II-Lys, now polymerization by transglycosylation would require expulsion of a carbanion which would be chemically highly disfavoured. Methylene lipid II-Lys was not a transpeptidase donor but was inhibitory (Figure S6e,f), consistent with polymerization as well as lipid II binding being essential for PBP1B transpeptidation. Congruent with this conclusion was that unpolymerizable candidate donors MurNac *meso*-DAP pentapeptide, undecaprenyl pyrophosphoryl MurNAc *L*-alanyl-γ-*D*-glutamyl-*L*-lysyl-*D*-alanyl-*D*-alanine (Lipid I-Lys) or undecaprenyl pyrophosphoryl MurNAc *L*-alanyl-γ-*D*-glutamyl-*meso*-DAP-*D*-alanyl-*D*-alanine (Lipid I-*meso*-DAP), also could not support transpeptidation (Figure S7b,c).

However, these data could not formally distinguish between transpeptidation inhibition arising from binding of methylene lipid II-Lys to either the transglycosylase or transpeptidase active sites of PBP1B. Therefore, to confirm the essentiality of polymerization of lipid II for catalysis of transpeptidation, we evaluated the impact of hen egg white lysozyme which cleaves the β1-4 linkages between MurNAc-GlcNAc disaccharides of peptidoglycan polymers[1] on the transpeptidase activity of PBP1B. Lysozyme was a potent inhibitor of transpeptidase activity (Figure S6g), with an IC_{50} of 2.07 ± 0.09 μM (n=3). This observation was consistent with lipid II-Lys polymerization being a pre-requisite for transpeptidation.

As PBP1B polymerizes tetrapeptide precursors *in vivo*[25], which would be transpeptidase acceptors, we tested PBP1B transpeptidation with MurNac *meso*-DAP pentapeptide, Lipid I-Lys or Lipid I-*meso*-DAP as monomeric donors with undecaprenyl pyrophosphoryl GlcNAc-MurNAc *L*-alanyl-γ-*D*-glutamyl-*meso*-DAP-*D*-alanine (Lipid II-*meso*-DAP tetrapeptide; **S.1.2.4.2**; Tables S1 and S2; Figure S2) as a polymerisable acceptor. No *D*-alanine release occurred (Figure S7b,c) suggesting that the necessity for donor polymerization could not be supplanted by a polymeric acceptor.

To further explore PBP1B transpeptidation with polymerized donors, we added lipid II-Lys and *Staphylococcus aureus* monofunctional transglycosylase (the activity of which we confirmed by SDS-PAGE analysis of polymerization of lipid II-$^{\varepsilon}$N-dansyl-Lys; **S.1.2.7.**; Figure S7d) to assays prior to PBP1B or MurNAc *meso*-DAP pentapeptide. Considerably less transpeptidation was observed (Figure S7a), suggesting PBP1B only accepted polymeric transpeptidation donor generated on itself.

Characterization of *E. coli* PBP1B transpeptidase donor and acceptor kinetics and substrate specificity. The dependence of PBP1B transpeptidation rate on lipid II-*meso*-DAP was sigmoidal, could not be linearised by replotting the data as a half reciprocal plot (Figure 3a and insert) or fitted to the Michaelis Menten equation:

$$v_o = \frac{V_{max}^{App}.[S]}{K_m^{App} + [S]} \qquad \text{Equation 1}$$

but it could be fitted to an equation describing utilization of two moles of substrate/mol enzyme/turnover:

$$v_o = \frac{V_{max}.[S]^2}{K_{m1}.K_{m2} + K_{m1}.[S] + [S]^2} \qquad \text{Equation 2}$$

This suggested two values of K_m (7 ± 3 μM and 9 ± 7 μM) with a k_{cat} of 160 ± 10 min^{-1}. LCMS analysis (Figure 2c) argued against significant contribution of *D,D*-carboxypeptidase activity to these data. Therefore, these K_m values might represent lipid II-*meso*-DAP binding to the transpeptidase donor and acceptor sites. To explore this further, exclusively donor and acceptor substrates were required.

Characterization of transpeptidase donor recognition. Using lipid II-Lys as an exclusive transpeptidase donor[19,20] with 2 mM *D*-lactate as acceptor, PBP1B transpeptidation was hyperbolically dependent on lipid II-Lys (Figure 3b) as was evident from the linear half reciprocal plot of the data (Figure 3b insert) and fitted the Michaelis Menten equation yielding a K_m^{App} of 8.7 ± 0.6 μM and k_{cat}^{App} of 2.72 ± 0.06 min^{-1}. This suggested now one donor:PBP interaction was required for transpeptidation, contrasting with lipid II-*meso*-DAP utilization, which required two such interactions. Similarly, PBP1B transpeptidation was hyperbolically dependent on lipid II-Lys with more complex acceptors e.g. MurNAc *L*-alanyl-γ-*D*-glutamyl-*meso*- DAP (MurNAc *meso*-DAP tripeptide; Figure 3c).

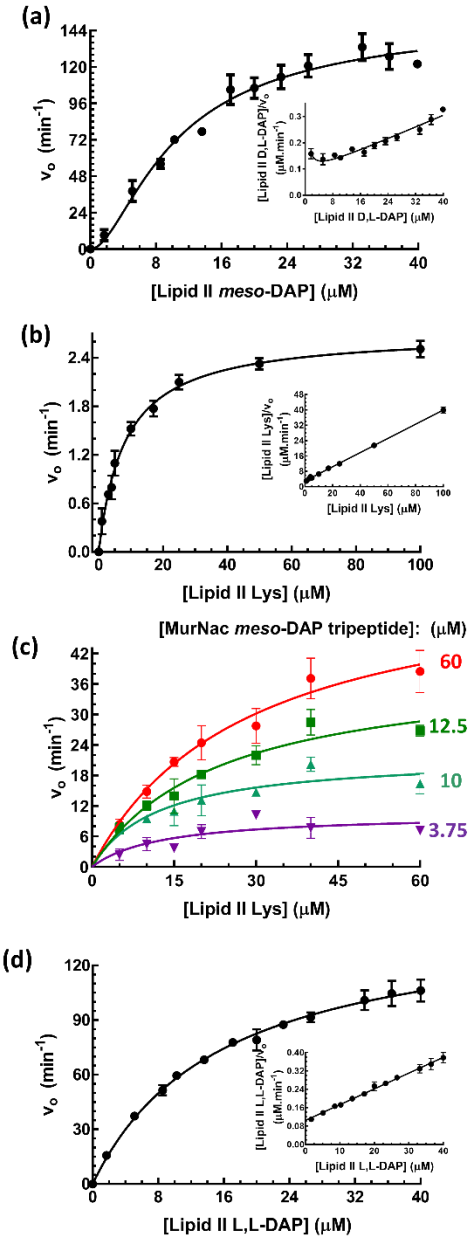

Figure 3: Dependence of initial rates of D-alanine release from lipid II donors. Error bars are ± S.D. of 4 or 3 observations for data in panels **(a)** and **(b)-(d)** respectively. **(a)** *Dependence of initial rate of D-alanine release by PBP1B on lipid II-meso-DAP.* Initial rates following A_{555} were initiated by 5.5 nM PBP1B. Controls replaced lipid with 0.1% (v/v) Triton X-100. Main panel: initial velocity vs [lipid II-*meso*-DAP], fitted to equation 2 in the text. Insert is the data as a half reciprocal plot ([lipid II-*meso*-DAP]/v_o vs [lipid II-*meso*-DAP]). **(b)** *Dependence of initial rate of transpeptidation between lipid II-Lys and D-lactate by PBP1B.* $A_{555\ nm}$ was followed and at 2 minutes and 8 minutes, 5.5 nM PBP1B and 2 mM D-lactate acceptor were added respectively. Controls omitted donor lipid. Main panel is initial velocity vs [lipid II-Lys], fitted to Equation 1in the text. The insert is the data as a half reciprocal plot. **(c)** *Dependence of initial rate of transpeptidation between lipid II-Lys and MurNAc meso-DAP tripeptide by PBP1B.* $A_{555\ nm}$ was followed for 2 minutes after which time, 9.6 nM PBP1B was added. $A_{555\ nm}$ was followed for a further 6 minutes, when lipid II-Lys was then added. The experiment was carried out at 3.75, 10, 12.5 and 60 μM MurNAc *meso*-DAP tripeptide acceptor. Controls omitted acceptor. Data were fitted to equation 1 in the text. **(d)** *Dependence of initial rate of D-alanine release by PBP1B on lipid II-L,L-DAP.* Initial rates followed as A_{555}were initiated by 6.2 nM PBP1B. Control assays replaced the lipid substrate with 0.1% (v/v) Triton X-100. Main panel is initial velocity vs [lipid II-*L*,*L*-DAP], fitted to equation 1 in the text. The insert is the data as a half reciprocal plot.

To further probe transpeptidase donor recognition, we synthesised lipid II-Lys analogues where N$^{\varepsilon}$-biotinyl L-lysine, N$^{\varepsilon}$-dansyl *L*-lysine, N$^{\varepsilon}$-methyl *L*-lysine, 5-hydroxy *L*-lysine or *L*-arginine replaced lysine (**S.1.2.4.1**; Tables S1 and S2, Figure S1). All lipids were donors (Figure S8). Lipid II-Arg and lipid II-N$^{\varepsilon}$-biotinyl-Lys were at least as active as lipid II-Lys as donors. However, methylation, hydroxylation or dansylation of the donor lysine attenuated activity

***E. coli* PBP1B transpeptidase donor recognition depends upon the glutamyl-α-carboxyl.** To characterize PBP1B donor recognition, we replaced *D*-glutamate of lipid II-Lys with *D-iso*-glutamine (amidated lipid II-Lys, **S.1.2.4.1**; Tables S1 and S2, Figures S1 and S9a) as found in Gram positive organisms[26]. As a PBP1B transpeptidase donor, amidated lipid II-Lys failed to support activity (Figure S9b) suggesting the glutamyl carboxyl was a key recognition element. Consequently, we established mass spectrometrically that amidated-lipid II-Lys supported transglycosylase activity (Figure S9c and d). Thus, the α-glutamyl carboxyl was key for transpeptidase donor recognition.

***E. coli* PBP1B transpeptidase donor recognition is stereoselective for the fifth position *D*-alanine.** To probe PBP1B transpeptidation stereochemistry at the donor C-terminus, we attempted, but failed to continuously couple *L*-alanine release from transpeptidation between lipid II-Lys with an *L*-alanyl-γ-*D*-glutamyl-*L*-lysyl-*D*-alanyl-*L*-alanine stem peptide (Lipid II-Lys (*L*-Ala) **S 1.2.4.1**; Tables S1 and S2, Figure S1) and MurNAc *meso*-DAP pentapeptide to alanine racemase (Figure S10c), despite the ability of PBP1B to polymerise this donor by transglycosylation (Figure S10a,b). Similarly, Lipid II-Lys (*L*-Ala) did not inhibit PBP1B transpeptidation (Figure S10c). To enhance assay sensitivity we reacted PBP1B with lipid II-Lys (*L*-Ala) for an hour prior to *L*-alanine assay. However, this approach failed to detect *L*-alanine release although *D*-alanine release from lipid II-Lys was detectable in this manner (Figure S10di and S10dii). This suggested donor recognition required a C-terminal *D*-stereo-centre.

Stereoisomerization of the ε-carboxyl of the donor *meso*-DAP residue stimulates *E. coli* PBP1B carboxypeptidase activity. Although we showed the ε-DAP carboxyl is dispensable for transpeptidase donors of *E. coli* PBP1B (Figure 1d,e), its stereochemistry profoundly affects peptidoglycan structure[27]. Therefore, we determined if lipid II-*L*,*L*-DAP, the stereoisomer of lipid II-*meso*-DAP was a transpeptidase donor. Lipid II-*L*,*L*-DAP (**S.1.2.4.1**; Table S1 and S2; Figure S1) supported rapid acceptor-independent evolution of *D*-alanine. We confirmed this with lipid II-*L*,*L*-DAP synthesised using *meso*-DAP dehydrogenase (**S.1.2.4.1**), to discount lipid II-*meso*-DAP contamination. PBP1B-catalysed *D*-alanine release kinetics were now hyperbolically dependent on lipid II-*L*,*L*-DAP (Figure 3d and insert) and could be explained by one K_m value, whereas those of lipid II-*meso*-DAP involved two such values.

Was PBP1B now acting as a *D,D*-carboxypeptidase ? Examination of the products formed by PBP1B from lipid II-*L,L*-DAP and lipid II-*meso*-DAP by LCMS and LCMSMS showed a 6.44-fold increase in the rate of synthesis of *D,D*-carboxypeptidase product GlcNAc-MurNAc *L*-alanyl-γ-*D*-glutamyl-DAP-*D*-alanine from lipid II-*L,L*-DAP (Figure 4b, confirmed by LCMSMS, Figure S3b; Table S4) relative to that of lipid II-*meso*-DAP. Concurrently there was an 8.8 fold decrease in the initial rate of transpeptidation (Figure 4a). LCMSMS (Figure S11a; Table S3) confirmed the residual transpeptidation of lipid II-*L,L*-DAP. This represented a 57-fold increase in the carboxypeptidation to transpeptidation ratio on inversion of the lipid II-DAP ε-carbon from a *D* to an *L* configuration.

If *L,L*-containing donors biased *E. coli* PBP1B towards *D,D*-carboxypeptidation, we speculated the donor peptide *L,L*- DAP *L*-ε-amino group might react with the ester between the *E. coli* PBP1B transpeptidase active site serine and the donor tetrapeptide. Therefore we assessed the impact of N-acetylation of the DAP ε-amino group of lipid II-*L,L*-DAP (termed lipid II-*L,L*-$^{\varepsilon}$NAc-DAP; **S.1.2.4.1**; Table S1 and S2; Figure S1) on PBP1B activity. *D*-Alanine release now depended upon MurNAc *meso*-DAP pentapeptide as an acceptor suggesting suppression of *D,D*-carboxypeptidase with restoration of transpeptidase activity. The transpeptidation rate (20 μM both substrates, 38 ± 3 min^{-1} (n = 3)) compared favourably with rates determined identically with 20 μM lipid II-Lys and MurNAc *meso*-DAP pentapeptide (27 ± 2 min^{-1} n=3).

Restoration of transpeptidation by lipid II-*L,L*-DAP N-acetylation was confirmed by LCMS (Figure 4c and cii). We detected the lipid II-*L,L*-$^{\varepsilon}$NAc.DAP/MurNAc *meso*-DAP pentapeptide transpeptidation product: GlcNAc-MurNAc *L*-alanyl-γ-*D*-glutamyl-*L,L*-$^{\varepsilon}$Nac-DAP-*D*-alanyl donor stem linked to the ε-amine of the *meso*-DAP of the MurNAc *meso*-DAP pentapeptide acceptor (expected/observed $(m+2H^+)/2$ = 886.38/ 886.38, for all anomer peaks). We also observed the corresponding product of lipid II-*meso*-$^{\varepsilon}$NAc-DAP (**S.1.2.4.1**; Table S1 and S2; Figure S1) and MurNAc *meso*-DAP pentapeptide (Figure 4c and ci; (expected/observed $(m+2H^+)/2$ = 886.38/886.38, for all anomer peaks). LCMSMS confirmed the structure of the lipid II-*L,L*-$^{\varepsilon}$NAc.DAP/MurNAc *meso*-DAP pentapeptide transpeptidation product (Figure S11b; Table S7). These data suggested orientation of the ε-amino group of the DAP moiety controlled the catalytic pathway(s) followed by the PBP1B transpeptidation site.

Characterization of transpeptidase acceptor recognition by truncation of the structure of Lipid II-*meso*-DAP. All acceptor (Table S1, S2 and Figure S2) dependencies of activity were hyperbolic (Figure S12a-j). Although the precision of the estimates of acceptor K_m and consequently k_{cat}/K_m for lipid II-meso-DAP (9 ± 7 μM and 20 ± 10 $min^{-1}.\mu M^{-1}$ respectively) was low, all acceptors containing *meso*-DAP were significantly active where truncation of lipid II-*meso*-DAP acceptor to Lipid I-*meso*-DAP and MurNAc *meso*-DAP pentapeptide respectively reduced the k_{cat}^{App}/K_m^{App} 8 ± 6- and 6 ± 5-fold (Table 1). C-terminal *D*-alanine deletion from lipid II-*meso*-DAP or MurNAc *meso*-DAP pentapeptide to generate Lipid II-*meso*-DAP tetrapeptide or MurNAc *L*-alanyl-γ-*D*-glutamyl-*meso*-DAP-*D*-alanine (MurNAc *meso*-DAP tetrapeptide), caused a 4 ± 2 - or 3 ± 2-fold drop in k_{cat}^{App}/K_m^{App} respectively relative to that of lipid II-*meso*-DAP (Table 1). Truncation of Lipid II *meso*-DAP to MurNAc *meso*-DAP tripeptide, reduced the k_{cat}^{App}/K_m^{App} for this substrate 8 ± 6-fold relative to that of lipid II-*meso*-DAP (Table 1). Truncation to MurNAc *L*-alanyl-γ-*D*-glutamate (MurNAc *L*-Ala-γ-*D*-Glu) inactivated the acceptor, consistent with loss of the *meso*-DAP ε-amino group.

The *D*-alanine analogues *D*-lactate (Table 1, Figure S12(i)) and the antibiotic *D*-cycloserine were acceptors that exchanged the donor C-terminal amino acid of lipid II-Lys from *D*-alanine to a *D*-lactyl or *D*-cycloseryl moiety. The k_{cat}^{App}/K_m^{App} for *D*-lactate dropped 3000 ± 2000-fold relative to that of lipid II-*meso*-DAP (Table 1). The *D*-cycloserine transpeptidase kinetics required substitution of *Rhodotorula gracilis D*-amino acid oxidase with the porcine kidney enzyme to reduce control rates in the presence of D-cycloserine to tolerable levels. Now, we were able to obtain rates at 50 μM and 100 μM *D*-cycloserine (which were inhibited by 50μM moenomycin) to generate preliminary estimates of k_{cat}^{App}, K_m^{App} and k_{cat}^{App}/K_m^{App} of 5.79 min^{-1}, 64.3 μM and 0.090 $min^{-1}\mu M^{-1}$ respectively, suggesting *D*-cycloserine was 20-fold more efficient than *D*-lactate as an acceptor, albeit that lipid II-*meso*-DAP was by far the preferred substrate (Table 1). That lipid II-Lys (*L*-Ala) was not a PBP1B donor led us to test *L*-alanine as an acceptor, where we observed the k_{cat}^{App}/K_m^{App} for this *L*-amino acid to be 13 ± 1-fold lower than that of *D*-lactate (Table 1; Figure S12i,j).

Identification of the ε-carboxyl of the *meso*-DAP residue as an essential peptidoglycan acceptor recognition element. The majority of recognition of the acceptor lay between the muramyl and diaminopimelyl moieties. Therefore, were the *D*-glutamyl α-carboxyl or *meso*-DAP ε-carboxyl groups of the stem peptide acceptor recognised by PBP1B? Considering k_{cat}^{App}/K_m^{App} values, substitution of iso-glutaminyl for isoglutamyl residues (denoted with the suffix NH_2) within any MurNAc *meso*-DAP acceptor (**S.1.2.4.2**; Tables S1 and S2; Figure S2) did not substantially affect PBP1B transpeptidation (Table 1; Figure S12c-h). Therefore, the α-glutamyl carboxyl negative charge was not recognised. Consistent with this, MurNAc dipeptide was not a PBP1B inhibitor. To probe the contribution of the *meso*-DAP ε-carboxyl to acceptor recognition, transpeptidation of lipid II-Lys with lipid I-Lys as acceptor was assayed. Unlike lipid I-*meso*-DAP, lipid I-Lys was unreactive, illustrating the importance of the *meso*-DAP ε-carboxyl in transpeptidase acceptor recognition.

We further probed the impact of acceptor DAP ε-carboxyl and amino group stereochemistry on transpeptidation. Lipid II-*L,L*-DAP tetrapeptide was not active as an acceptor at 20μM (Figure 4d), whereas lipid II-*meso*-DAP tetrapeptide was (Figure 4e). LCMS (Figure 4f) showed formation of the transpeptidation product GlcNAc-MurNAc *L*-alanyl-γ-*D*-glutamyl-*L*-lysyl-*D*-

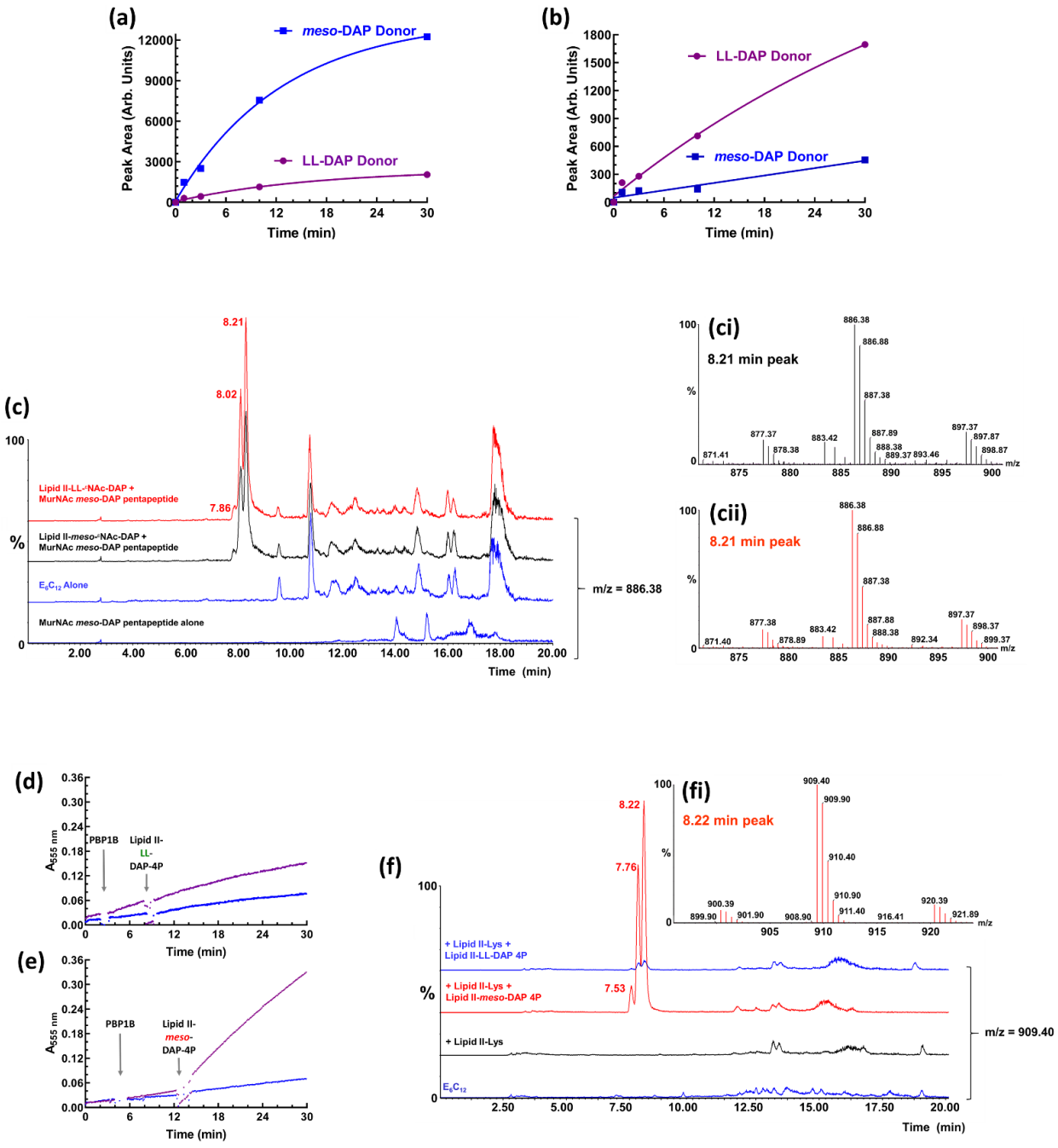

Figure 4: Analysis of the effect of donor and acceptor DAP stereoisomerization on *E. coli* PBP1B transpeptidation and carboxypeptidation. **(a)** *LCMS time course of transpeptidation or* **(b)** *carboxypeptidation of lipid II-meso or L,L-DAP.* 9.6 nM PBP1B was incubated with 20 μM lipid II *meso* or *L,L*-DAP. Products were digested and subjected to LCMS (**S.1.2.3.2.1**). Peak areas from extracted ion chromatograms for the transpeptidase or carboxypeptidase products ((m+2H$^+$)/2 = 996.92 or (m+H$^+$)/1 = 940.40) were plotted vs. time. **(c)** *LCMS of PBP1B transpeptidation with MurNAc meso-DAP pentapeptide acceptor and lipid II-meso or L,L-ᵉNAc-DAP.* 9.6 nM PBP1B was incubated ±20 μM MurNAc *meso*-DAP pentapeptide ± 20 μM lipid II-*meso*- or *L,L*-ᵉNAc-DAP. –lipid II controls replaced the lipid with hexaethylene glycol dodecyl ether (E_6C_{12}). Transpeptidase product extracted ion chromatograms ((m+2H$^+$)/2 = m/z of 886.38) are shown: *MurNAc meso-DAP pentapeptide alone*; *E6C12 alone*; *Lipid II-meso-ᵉNAc DAP + MurNAc meso-DAP pentapeptide* or *Lipid II-L,L-ᵉNAc DAP + MurNAc meso-DAP pentapeptide*. **(ci)** and **(cii)**: Transpeptidation product mass spectra (expected (m+2H$^+$)/2 for *meso* and *L,L* species = observed = 886.38). **(d)** *D-alanine release from lipid II-Lys donor using Lipid II-L,L-DAP tetrapeptide or* **(e)** *Lipid II-meso-DAP tetrapeptide as acceptor*. 20 μM lipid II-Lys (purple trace) or Triton X-100 (blue trace) was added at zero minutes. 6.17 nM PBP1B and 20 μM lipid II-*L,L*- or *meso*-DAP tetrapeptide (denoted as Lipid II LL-DAP-4P or Lipid II-*meso*-DAP-4P) or 0.1% (v/v) Triton X-100 was added as indicated. A_{555} was followed. **(f)** *LCMS of transpeptidation with lipid II-DAP tetrapeptide and lipid II-Lys:* 9.6 nM PBP1B was incubated with 20 μM lipid II-*meso*-or *L,L*-DAP tetrapeptide and 20 μM lipid II-Lys. LCMS (**S.1.2.3.2.1**) followed elution of 909.40 m/z (expected (m+2H$^+$)/2 for the transpeptidase product). Controls + PBP1B alone (trace ***E6C12***), - acceptor (trace ***+Lipid II-Lys***), or complete reactions (traces ***Lipid II-Lys + Lipid II-meso-DAP 4P*** or ***Lipid II-Lys + Lipid II-L,L-DAP 4P***) are shown. Transpeptidation product anomer retention times are in red. (**4fi**) is the mass spectrum of the *meso*-DAP transpeptidation product (exp. (m+2H$^+$)/2 for *meso* and *L,L* species = that observed for both = 909.40).

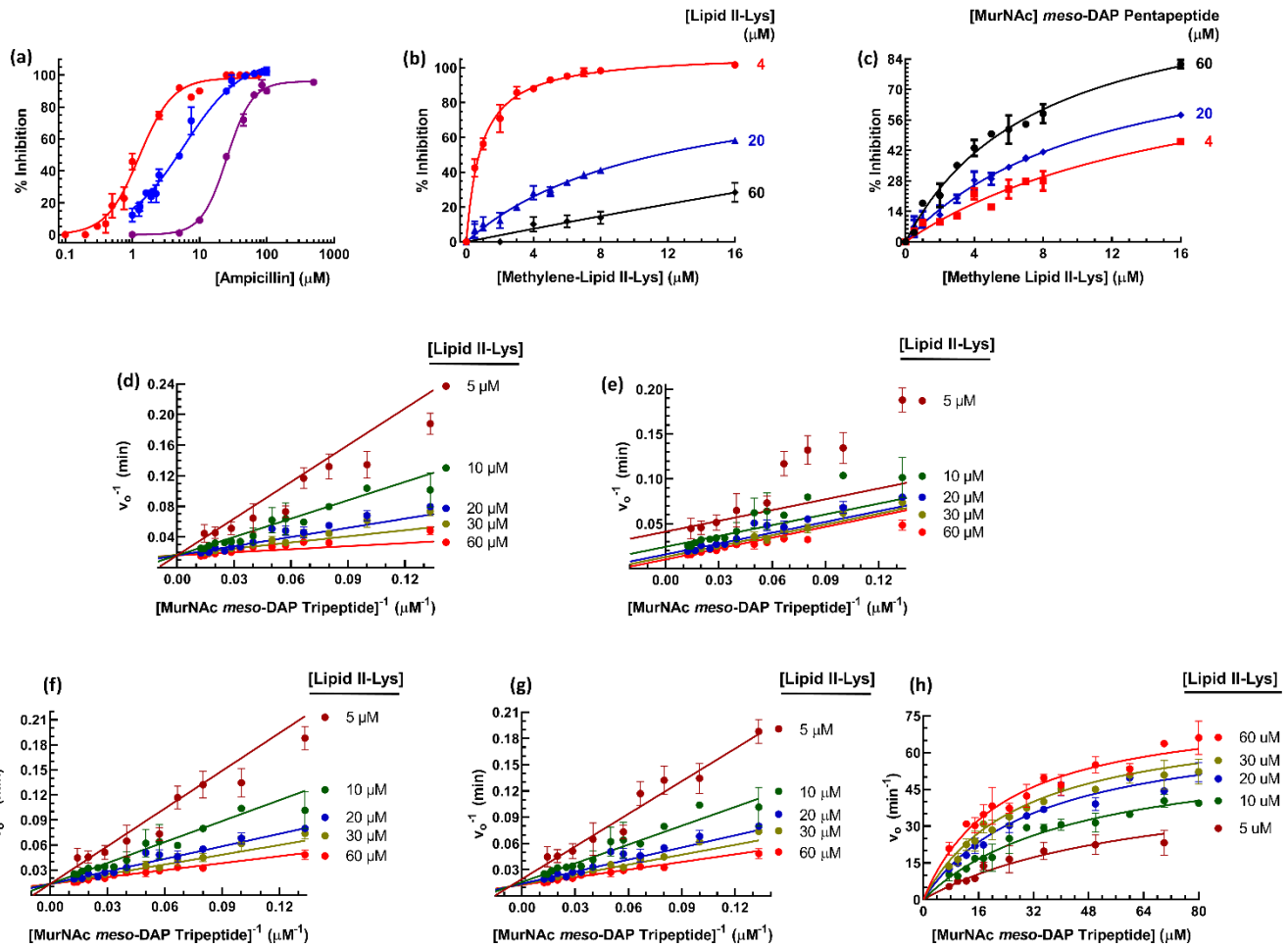

Figure 5: β-lactam and donor analogue inhibition and steady state kinetics indicate simultaneous binding of donor and acceptor occurs prior to *E. coli* PBP1B transpeptidation. Errors are ± S.D. (n=3) for data in panels **(a)-(h)**. **Panel (a)** *Impact of donors and acceptors on PBP1B inactivation by ampicillin.* Assays contained all components except PBP1B, lipid II-Lys and acceptor. Parallel assays were run without ampicillin. Remaining activity at 555 nm was followed after the last (8 minute) addition: ***Preincubation with lipid II donor (maroon trace)***: 20 μM lipid II-Lys, 8.49 nM PBP1B and 10 μM MurNAc *meso*-DAP tripeptide were added at 0, 2 and 8 minutes respectively. ***Preincubation with MurNAc meso-DAP tripeptide acceptor (blue trace)***: 10 μM MurNAc *meso*-DAP tripeptide, 8.49 nM PBP1B and 20 μM lipid II-Lys donor were added at 0, 2 and 8 minutes respectively. ***Preincubation without substrate (red trace)***: 8.49 nM PBP1B was added at 2 minutes. 20 μM lipid II-Lys and 10 μM MurNAc *meso*-DAP tripeptide were added simultaneously at 8 minutes. **Panel (b)** *Impact of lipid II-Lys donor on inhibition of PBP1B by methylene lipid II-Lys.* All components except PBP1B and MurNAc *meso*-DAP pentapeptide were present at time zero. At 2 and 8 minutes, 9.6 nM PBP1B and 20 μM MurNAc *meso*-DAP pentapeptide were added to initiate transpeptidation. **Panel (c)** *Impact of MurNAc meso-DAP pentapeptide acceptor on inhibition of E. coli PBP1B by methylene lipid II-Lys.* All components excluding PBP1B and MurNAc *meso*-DAP pentapeptide were present at time zero. At 2 and 8 minutes, 9.6 nM PBP1B and MurNAc *meso*-DAP pentapeptide were added to initiate transpeptidation. **Panels (d)** to **(g)** *Double reciprocal plot of the impact of lipid II-Lys donor on the dependence of E. coli PBP1B transpeptidation on MurNAc meso-DAP tripeptide.* At 2 and 8 minutes, 9.6 nM PBP1B and 7.5-80 μM MurNAc *meso*-DAP tripeptide were added to initiate transpeptidation with 5-60 μM lipid II-Lys. Data (initial velocity (v_o) vs [MurNAc *meso*-DAP tripeptide] at constant [lipid II-Lys]) were globally fitted to equations describing an ordered rapid equilibrium mechanism with MurNAc *meso*-DAP tripeptide as the first binding substrate (Panel d), a ping pong mechanism with lipid II-Lys as the first substrate (Panel e), an ordered rapid equilibrium mechanism with lipid II-Lys as the first binding substrate (panel f) and a random rapid equilibrium mechanism (Panel g) (Equations S3, S4, S2 and 3 respectively; Figure S13). Double reciprocal relationships were then calculated from these fits and superimposed over the data. **Panel (h)** Initial velocity data superimposed over theoretical curves of v_o vs. [MurNAc *meso*-DAP tripeptide] at various [lipid II] computed with Equation 3 and corresponding constants in the text.

alanyl donor linked to the ε-amine of the *meso*-DAP of the acceptor GlcNAc-MurNAc *L*-alanyl-γ-*D*-glutamyl-*meso*-DAP-*D*-alanine (expected/ observed $(m+2H^+)/2$ = 909.40/ 909.40, for all three anomer peaks). In contrast, virtually no product was generated from lipid II-*L*,*L*-DAP tetrapeptide acceptor consistent with the spectrophotometric data (Figure 4d,e), showing a *D*-configured DAP ε-carboxyl was essential for transpeptidase acceptor recognition.

Response of transpeptidation to β-lactam challenge suggests donor and acceptors bind to PBP1B independently. PBP1B is inactivated by β-lactam acylation of the transpeptidase active site serine[22,24]. Ampicillin inhibited PBP1B transpeptidation with an IC_{50} of 1.27 ± 0.06 μM which was increased to 26 ± 2 μM by pre-incubation with 20 μM lipid II-Lys donor, and to 4.1 ± 0.3 μM by pre-incubation with 20 μM MurNAc *meso*-DAP tripeptide acceptor (Figure 5a; chosen as unlikely to compete

with the β-lactam for the donor site due to truncation of *D*-alanyl-*D*-alanine). Protection of transpeptidation from β-lactam inhibition by either substrate suggested independent transpeptidase donor or acceptor site binding by lipid II-Lys (or its polymer) and MurNAc *meso*-DAP tripeptide.

PBP1B inhibition by a non-hydrolysable analogue of lipid II-Lys confirms binding of donor and acceptor to form a ternary complex with PBP1B. The ampicillin IC_{50} experiments suggested PBP1B bound both substrates. We used methylene lipid II-Lys as a donor analogue to confirm this result. Methylene lipid II-Lys was an inhibitor of transpeptidation with an IC_{50} of 0.9 ± 0.2 μM, 18.8 ± 0.8 μM and > 20 μM at 4, 20 and 60 μM lipid II-Lys respectively (Figure 5b). Thus the analogue competed with the donor for the transglycosylase and (albeit indirectly) for the transpeptidase sites of PBP1B. However, at 4, 20 and 60 μM MurNAc *meso*-DAP pentapeptide, respective IC_{50} values for methylene lipid II-Lys were 17 ± 5 μM, 12 ± 5 μM and 7.8 ± 0.9 μM (Figure 5c), suggesting mixed or uncompetitive inhibition by the analogue, that the acceptor bound PBP1B with or without lipid II-Lys donor at the transglycosylation site and that acceptor and donor could simultaneously bind PBP1B.

PBP1B employs a sequential transpeptidase mechanism with a ternary complex of donor, acceptor and PBP1B. MurNAc *meso*-DAP tripeptide acceptor bound to PBP1B without the donor (Figure 5a), consistent with donor and acceptor binding the active site prior to D-alanine release through donor acylation of the PBP[28]. We therefore examined the relationship between initial velocity of transpeptidation and donor concentration between 5 and 60 μM lipid II-Lys at MurNAc *meso*-DAP tripeptide acceptor concentrations between 7.5 and 80 μM.

Plots of velocity *versus* MurNAc *meso*-DAP tripeptide concentration at each lipid II-Lys donor concentration were hyperbolic. Fitting of the data to equations 3 and S2-4 by global non-linear regression using MATLAB 2017a (**S.1.2.8.**; Table S8) allowed rejection of equations describing rapid equilibrium Bi Bi ordered mechanisms where the acceptor bound before the donor (Equation S3; sum of squared errors; SSE, was 4547.84) and Ping Pong (Equation S4; SSE = 4021.19) mechanisms, where the most appropriate models based upon the SSE and the model correlation coefficient was a Bi Bi rapid random equilibrium mechanism (Equation 3; SSE = 2409.5; r^2 = 0.94) and an ordered rapid equilibrium mechanism (Equation S2; SSE = 2458.93; r^2 = 0.94; Table S8). The selection of these equations as most appropriate models of PBP1B transpeptidase kinetics is discussed further in **S.2.3.**

Visual inspection of the fits by plotting theoretical relationships of velocity *vs.* MurNAc *meso*-DAP tripeptide concentration (Figures S13 and 5h) and reciprocals thereof (Figures 5d-g) calculated from the constants extracted by global non-linear regression suggested the random rapid equilibrium model to be preferable over the other three models. However, statistically, MATLAB could not distinguish between the rapid equilibrium or ordered (donor first) model as SEE and r^2 parameters for both fits were essentially identical (Table S8). Nevertheless, our ampicillin and methylene lipid II-Lys inhibition data (Figure 5a-c) suggested independent binding of both acceptor and donor to the enzyme, and therefore equation 3 describing a random rapid random equilibrium mechanism[28] was deemed to be the most appropriate descriptor of the relationship between initial velocity of PBP1B transpeptidation and donor lipid II-Lys and MurNAc *meso*-DAP tripeptide concentrations (Figure 5h).

$$v_o = \frac{V_{max}.[LII].[M3P]}{\alpha.K_{LII}.K_{M3P} + \alpha.K_{LII}.[M3P] + \alpha.K_{M3P}.[LII] + [LII].[M3P]}$$

Equation 3

In equation 3, K_{LII} and K_{M3P} are the dissociation constants of donor and acceptor in the absence the co-substrate, α is the factor by which K_{LII} and K_{M3P} were modified by the co-substrate and V_{max} was the maximal velocity at infinite donor and acceptor concentration. Values were: k_{cat} = 84 ± 5 min^{-1}, K_{LII} = 25 ± 6 μM, K_{M3P} = 130 ± 80 μM, and α = 0.13 ± 0.09 μM. It should be noted however, that operation of either a Bi Bi random rapid equilibrium mechanism or an ordered Bi Bi *steady state* mechanism[28] could not be distinguished as these mechanisms share the same form of rate equation.

DISCUSSION

This paper describes the transpeptidation enzymology of *E. coli* PBP1B employing a kinetically competent continuous assay with polymerizable peptidoglycan substrates or fragments thereof that is sensitive, straightforward, robust, can characterize acceptor and donor-dependent kinetics and was validated by LCMS and LCMSMS. Importantly, this assay is of potential utility for 4,3- and 3,3-crosslinking transpeptidases[29], does not rely on laborious product purification[22,30-32], unnaturally reactive substrates[21,33] or unphysiological fluorescent substrates yielding uncharacterized products[34,35]. Two available radiochemical transpeptidation assays using natural substrates employ digestion of transpeptidation products followed either by HPLC[22] or SDS-PAGE[32] fractionation. Neither monitor PBP activity quantitatively compared to the assay reported here.

If PBP1B was incubated with donor, which it had the opportunity to polymerise by transglycosylation, the assay entered steady state immediately on addition of acceptor, (e.g. Figures 1e,f and 4e). Conversely, there was a discernible lag if the reaction was initiated by addition of donor (Figure 1a, 1d), which probably related to the time taken to accumulate polymer at the transpeptidase active site. Any pre-steady state lag accounted for consumption of less than 5% of the donor substrate in assays performed in this manner and therefore, initial rates were measured from the subsequent onset of steady state.

We observed low back ground rates of resorufin production in the presence of exclusive donor substrates such as lipid II-Lys, which comprised of mostly residual D,D-carboxypeptidase activity (e.g. Figure 1e and f). However even lower rates of absorbance change in the presence of ampicillin or just Triton X-100, or without D-amino oxidase (Figures 1d,e and f) were also observable, which could be attributable to back ground levels of auto-oxidation of amplex red[36].

Acceptor	Equation fitted	[Donor] (μM)	$[PBP1B]_{assay}$ (nM)	[Acceptor] range (μM)	k_{cat}^{App} ± S.D. (min^{-1})	K_m^{App} ± S.D. (μM)	k_{cat}^{App}/K_m^{App} ($min^{-1}\cdot\mu M^{-1}$)	n	r^2
Lipid II *meso*-DAP	2	2 - 39.9	5.5	2 - 39.9	160 ± 10	9 ± 7	20 ±10	4	0.972
Lipid II *meso*-DAP tetrapeptide	1	20	11.0	2 - 20	41 ± 1	9.7 ± 0.7	4.2 ± 0.4	3	0.994
Lipid I *meso*-DAP	1	20	11.0	2 - 35	42 ± 2	19 ± 2	2.2 ± 0.2	3	0.989
MurNAc *meso*-DAP Pentapeptide	1	20	11.0	1 - 50	110 ± 3	41 ± 2	2.7 ± 0.1	3	0.998
MurNAc *meso*-DAP Tetrapeptide	1	20	11.0	1 - 50	48.6 ± 0.5	8.1 ± 0.3	6.0 ± 0.2	3	0.998
MurNAc *meso*-DAP Tripeptide	1	20	11.0	1 - 100	76 ± 4	35 ± 4	2.2 ± 0.2	3	0.940
MurNAc *meso*-DAP Pentapeptide-NH_2	1	20	6.2	1 - 50	87 ± 4	24 ± 2	3.6 ± 0.4	3	0.980
MurNAc *meso*-DAP Tetrapeptide-NH_2	1	20	6.2	1 - 50	190 ± 10	46 ± 5	4.0 ± 0.5	3	0.989
MurNAc *meso*-DAP Tripeptide-NH_2	1	20	6.2	1 - 50	108 ± 9	29 ± 5	3.7 ± 0.7	3	0.948
D-Lactate	1	20	11.0	500 – 50,000	25.1 ± 0.3	5000 ± 300	0.0051 ± 0.0003	3	0.995
L-Alanine	1	20	8.5	2000-92,500	68 ± 4	170,000 ± 10,000	0.00040 ± 0.00004	3	0.997

Table 1: Specificity and kinetics of dependence of *E. coli* PBP1B transpeptidation on acceptor concentration. Assays were performed (Methods) with 1.97 μM LpoB. Where the substrate was lipid II-*meso*-DAP, the donor and acceptor concentrations were initially identical and data were fitted to Equation 2 in the text. Where lipid II-*meso*-DAP dependence was followed, control assays replaced lipid by 0.1% (v/v) Triton X-100. For all other acceptors, donor (20 μM lipid II-Lys) was added first, followed by PBP1B, followed by acceptor. Controls omitted donor at each [acceptor] and rates were fitted to Equation 1 in the text. Assays were performed in triplicate or quadruplicate (column n). Goodness of fit was quantified by correlation coefficient (r^2). Standard deviations for k_{cat}^{App}/K_m^{App} ratios were computed as in[64]

Our lipid II *meso*-DAP transpeptidation assay was directly proportional to PBP1B between 4-210 nM (Figure 1c). This was surprising because dimerization of PBP1B was previously observed with a K_D of 127 nM[22] (despite contradiction of this observation by seven crystal structures from two independent investigations[24,37]). The dimeric PBP1B transpeptidation activity was found to be greater than that of the monomeric protein[22] which would have been expected to cause the relationship between transpeptidation activity and protein concentration to deviate from the linearity seen in Figure 1c. However, the observations in[22] were made without substrates or LpoB, whereas our data was acquired with them and may not be comparable. Previously, activation of PBP1B transpeptidation by LpoB was reported as being less than two-fold[16-18,23,38]. However, the essentiality of LpoB in the absence of PBP1A or LpoA *in vivo*[16,17] was therefore inconsistent with its reported modest impact *in vitro*, which could be achieved *in vivo* by changes in PBP1B expression. Nevertheless, we have shown LpoB-activation of PBP1B great enough (Figure 1b), to be consistent with the *in vivo* essentiality of LpoB. The discrepancy between our LpoB data and[16-18,23,38] is likely because[16-18,23,38] did not follow initial rates, and so significantly underestimated LpoB-activation.

The only transpeptidase products detectable by LCMS and LCMSMS were dimeric donor:acceptor pairs. No lipid II *meso*-DAP transpeptidation products where three or four disaccharide peptides were linked were detected, even when carried out with one hundred times (1 μM) the amount of PBP1B used in the spectrophotometric assay. Previously, radiochemical HPLC-based assays detected these species as minor products by employment of micromolar PBP concentrations[8,22], however these assays were conducted over one hour, whilst our data was acquired from within the first 20 minutes of reaction, which may account for our inability to detect tri or tetrameric transpeptidation products.

Our non-polymerizable lipid II-Lys analogue - methylene lipid II-Lys bound PBP1B without transpeptidation (Figure S6e,f), indicating polymer extension predicated transpeptidation. We confirmed this finding by demonstrating the inhibition of transpeptidation by digestion of polymerised lipid II with lysozyme (Figure S6g). Methylene lipid II-Lys was a less potent inhibitor than moenomycin possibly because the latter mimics binding of a tetrasaccharide, making extensive interactions with residues in and beyond the transglycosylase donor site[24] whilst our analogue mimics only disaccharide binding to the transglycosylase acceptor site of PBP1B. Interestingly, prepolymerised transpeptidase donor did not support transpeptidation (Figure S7a) suggesting glycan polymer passage between transglycosylation and transpeptidation sites was only accessible by glycan polymerized on enzyme. This was consistent with[39] and[40] where lipid II polymerization by PBP1B in sphaeroplasts did not require polymeric peptidoglycan primer because of the ability of PBP1B to polymerize glycan chains *de novo*[22].

The efficiency of PBP1B lipid II *meso*-DAP transpeptidation (Table 1) was comparable with other peptidoglycan synthetic enzymes[41-45]. Thus PBP1B transpeptidation is unlikely to limit peptidoglycan synthesis. Crosslinking frequency in peptidoglycan[46] and PBP1B transpeptidation rates relative to transglycosylation[22] suggest the latter does not rate-limit the former. This agrees with our data and[24] where PBP1B

transglycosylation depends sigmoidally upon lipid II-Lys. If transglycosylation limited transpeptidation, sigmoid lipid II-Lys kinetics would characterize transpeptidation. However, this relationship was hyperbolic (Figure 3b,c) suggesting no such limitation, consistent with[22,24,46]. Hence the lipid II-*meso*-DAP kinetics in Figure 3a reflect transpeptidation of an identical acceptor and donor.

We identified the donor glutamyl-α-carboxyl as a PBP1B recognition element (Figure S9) in contrast to *Streptococcus pneumoniae* PBPs where α-amidation of D-glutamyl is recognised[35]. Like PBP1B, *E. coli* PBP6[47] similarly interacts with the donor α-glutamyl carboxyl. Donor stem peptide third position recognition was less specific. Various N^{ε} acyl-lysines could replace *meso*-DAP showing its *D*-ε-amino group was not recognised (Figure S8). Similarly, *E. coli* PBP6 had no interaction with the stem peptide lysine[47]. Acceptance of donors with *L*-lysine or *L*-arginine by PBP1B highlights the role of *E. coli* MurE, barring *L*-lysine or *L*-arginine incorporation into peptidoglycan in favour of *meso*-DAP[43,46,48,49].

Like *Streptomyces* R61 transpeptidase[50], *E. coli* PBP1B strongly discriminated against lipid II-Lys (*L*-Ala) or *L*-alanine as a donor or acceptor (Figure S10c,d(i)), suggesting the *D*-configuration of the donor C- and acceptor N-terminii was strongly favoured. *Streptomyces* R61 *D*,*D*-transpeptidase and *E. coli* PBP6 bind the substrate C-terminal *D*-alanine through numerous hydrogen bonds[47,51] congruent with the stereo-selectivity of *E. coli* PBP1B. Our synthesis of lipid II-Lys (*L*-Ala) (**S.1.4.2.1.**, Tables S1 and S2, Figure S1) showed peptidoglycan precursor synthesis could be corrupted by *D*-alanyl-*L*-alanine *in vitro*. The failure of *E. coli* PBP1B transpeptidase to interact with lipid II-Lys (*L*-Ala) and the fidelity of *D*-alanine-*D*-alanine ligase that precludes *D*-alanyl-*L*-alanine generation[52] may prevent corruption of peptidoglycan synthesis *in vivo*.

D-lactate and *D*-cycloserine were more efficient PBP1B acceptors than *L*-alanine (Table 1, Figure S12i,j). *D*-cycloserine utilization was curious, as there is no free α-carboxyl adjacent to the amine nucleophile of this molecule, which we had shown here to be a PBP1B acceptor recognition element. However, *D*-cycloserine utilization by *Streptomyces D*,*D*-transpeptidases is known[53,54] where it was accounted for by virtue of an appreciable negative charge on the carbonyl oxygen of the molecule α to its free amino group[54]. This would endow the antibiotic with α-amino acid-like properties explaining its recognition as an acceptor by PBP1B. The ability of PBP1B to utilise D-cycloserine may enhance β-lactam lethality by corrupting transpeptidation or preventing peptidoglycan precursor synthesis[55].

Lipid I *meso*-DAP was an *E. coli* PBP1B transpeptidation acceptor (Table 1, Figure S12a) but cannot be transglycosylated. Thus the lipid II flippase has to avoid lipid I *meso*-DAP transport to the outer face of the cell membrane to forestall competition with peptidoglycan acceptor strands for transpeptidation which would weaken peptidoglycan. MurJ/FtsW specificity is unknown[56] but may be important because the *E. coli* lipid I-*meso*-DAP : lipid II-*meso*-DAP ratio is 7:2[57].

The only PBP1B acceptor peptide element recognised was the *meso*-DAP carboxyl, consistent with accumulation of uncrosslinked lysine-containing stem peptides on *S. aureus* MurE over-expression in *E. coli*[19]. Our data and[19] suggest peptidoglycan disruption through replacement of *meso*-DAP with lysine could be avoided by discrimination against lysine-containing acceptors by PBP1B and other PBPs.

The correct orientation of the DAP acceptor ε-carboxyl was as essential here (Figure 4d,e), as it is *in vivo* for transpeptidation[27]. The *meso* to *L*,*L* re-orientation of the donor DAP ε-amino group might facilitate binding of water between it and the PBP1B-esterified carbonyl of the donor *D*-alanyl residue, promoting carboxypeptidation (Figure 4b, S3a, Table S4). Consistent with this, *E. coli* PBP5 may use water to protonate *D*-alanine during *D*,*D*-carboxypeptidation[58]. That lipid II *L*,*L*-DAP ε-N-acetylation restored donor transpeptidation (Figure 4c, S11b, Table S7) indicated orientation of this amine and/or a water might control the PBP1B transpeptidation:carboxypeptidation ratio. Discrimination of PBP1B against crosslinking *L*,*L*-DAP-peptides might ensure *L*,*L*-DAP residues evading MurE specificity would be uncrosslinked, preserving *D*,*D*-stereochemistry of 4,3 peptidoglycan crosslinking and cell wall structure. We propose lipid II *L*,*L*-DAP enhancement of carboxypeptidation and discrimination against *L*,*L*-DAP acceptors constitutes an editing mechanism maintaining peptidoglycan stereochemistry if MurE fails to exclude *L*,*L*-DAP[27].

Peptidoglycan synthesis is targeted by β-lactam-acylation of PBPs[3,4]. Here, lipid II-Lys protected *E. coli* PBP1B transpeptidation from ampicillin (Figure 5a), suggesting β-lactam sensitivity was attenuated by peptidoglycan precursor competition for the PBP1B transpeptidation site. Consistent with this is donor-promoted relief of *Streptomyces* R61 *D*,*D*-carboxypeptidase-transpeptidase penicillin V inhibition[59]. Also relevant is the penicillin tolerance of stationary phase *E. coli*[60] possibly due to reliance on *L*,*D*-transpeptidase-catalysed 3,3 crosslinking[25] and peptidoglycan precursor accumulation competing with penicillin for the PBP active sites.

Muramyl *meso*-DAP tripeptide also attenuated ampicillin inhibition (Figure 5a), suggesting acceptor alone bound *E. coli* PBP1B. Similarly, *Streptomyces* R61 *D*,*D*-transpeptidase inhibition by penicillin V was weakened by a *meso*-DAP acceptor[59]. Methylene lipid II-Lys or ampicillin inhibition and our kinetic analysis of PBP1B (Figure 5a-h) suggested transpeptidase acceptor and transglycosylase/transpeptidase donor were bound as a ternary complex pre-transpeptidation, relating transglycosylase site lipid II binding to transpeptidase site acceptor binding. A related complex was proposed by Frere *et al.*[61,62] for *Streptomyces* R61 transpeptidase.

The reciprocal increase of the affinity of PBP1B for donor in the presence of acceptor and *vice versa* where here, αK_{LII} <

K_{LII} and $\alpha K_{M3P} < K_{M3P}$, as revealed by our kinetic mechanistic studies (Figure 5d-h) was consistent with acceptor-mediated increase in inhibitory potency of methylene lipid II-Lys (Figure 5c). Although our kinetic data were most consistent with PBP1B transpeptidation proceeding *via* a random rapid equilibrium kinetic mechanism (**S.2.3.;** Table S8, Figures 5d-g and S13), discrimination between this and an ordered steady state mechanism (which has the same form as equation 3[28]) will have to await more extensive product inhibition studies.

We observed detectable amounts of PBP1B-catalysed D-alanine release from lipid II-Lys alone (Figure S5b and Table S6). Although this is consistent with donor binding within a random or an ordered mechanism of catalysis, this activity was very low (e.g. Figure 1e,f and 4e), relative to PBP1B transpeptidation. Therefore, clearly the formation of a ternary complex of donor and acceptor with enzyme was obligatory for full expression of donor acylation as reported by D-alanine release. Our data suggest PBP1B avoids loss of donor peptides through unnecessary *D,D*-carboxypeptidation, maintaining efficiency of peptidoglycan synthesis (Figure 1e,f, Figure S5b). Our data (Figure 5a-h) are consistent with transglycosylation generating polymer, which with a bound acceptor, may be diverted to the transpeptidation site. Our data open up the possibility of generating potent PBP inhibitors incorporating aspects of both donor and acceptor substrates.

CONCLUSIONS

In this paper we have developed a continuous spectrophotometric method for the analysis of *E. coli* PBP1B activity. Although this has potential utility in the search for new antimicrobials that target PBPs, this technique was instrumental in uncovering hitherto undiscovered interactions between the enzyme and its peptidoglycan substrates responsible for recognition of peptidoglycan strands that would facilitate their successful crosslinking by transpeptidation. We also observed effective discrimination against stereochemically erroneous peptidoglycan substrates whose incorporation might compromise peptidoglycan synthesis, an observation whose physiological significance is underscored by the fact that *L,L*-DAP is the direct precursor of *meso*-DAP *in vivo*[27]. The findings reported here also addressed the impact of competing peptidoglycan precursors on the sensitivity of a β-lactam antibiotic for its target. This implies that flux through the peptidoglycan pathway may in part control the antibacterial killing exerted by these antibiotics and point to potential utility of co-administration of drugs that target not only PBP transpeptidases but also the enzymes that supply their donor substrates. Finally, it is an aspiration that the technology developed with respect to the generation of the peptidoglycan substrates used in this study might provide a useful resource supporting research in the field of bacterial cell wall synthesis in or beyond the context of antibiotic development.

METHODS

Spectrophotometric PBP1B Assays. The *E. coli* PBP1B transpeptidase assay was designed to follow PBP-catalysed release of *D*-alanine which was oxidised by *D*-amino acid oxidase producing hydrogen peroxide which was consumed by horse radish peroxidase, which with the chromogen amplex red, formed the dye resorufin (7-hydroxy-3H-phenoxazin-3-one), to establish a continuous assay for PBP activity. Where assays involved release of *L*-alanine, its conversion to *D*-alanine by alanine racemase, facilitated its detection by the *D*-amino acid oxidase/horse radish peroxidase couple. Coupling enzymes (*D*-amino acid oxidase, horse radish peroxidase, alanine racemase) were assayed as described in the **S.1.2.6.** Analysis of enzyme kinetic data was performed using GraphPad Prizm vers. 8 or MATLAB 2017a (**S.1.2.8.**).

Continuous and discontinuous spectrophotometric *E. coli* PBP1B transpeptidation activity assay. All spectrophotometric measurements were performed using a Cary 100 UV/vis spectrophotometer equipped with a 12-place Peltier thermostatically controlled cell changer (Agilent). Data were collected at 30°C using Hellma 1 cm pathlength micro quartz cuvettes with blacked out faces apart from an 8 mm x 2 mm window. Data were acquired every 0.1 seconds, with the spectrophotometer operating with a 1 cm slit bandwidth. The assay was configured to follow *D*-alanine release continuously in a final volume of 175 µl to 200 µl of 50 mM *bis*-Tris propane pH 8.5, 20 mM $MgCl_2$, 0.13% (v/v) Triton X-100, 50 µM amplex Red, 36.1 unit (U).ml^{-1} *R. gracilis D*-amino acid oxidase, 14.3 $U.ml^{-1}$ horse radish peroxidase (units as defined in **S.1.2.6.1.** and **S.1.2.6.3.**), 1.97 µM LpoB, lipid II donor, acceptor (both as specified in the text), and *E. coli* PBP 1B freshly diluted into 25 mM Tris, 0.2% (v/v) Triton X-100, 10% (v/v) glycerol pH 7.5. Assays were pre-incubated with either donor or acceptor for two minutes, at which point, the PBP was added. After a further six minutes, the final assay component (acceptor or donor) was added to initiate transpeptidation. Assays followed the increase in absorbance of resorufin at 555 nm (Resorufin $\varepsilon_{1cm,\ 555\ nm}$ = 54,000 $M^{-1}.cm^{-1}$[63]).

To follow *L*-alanine release in real time, the above continuous assay was additionally supplemented with 15.01 $U.ml^{-1}$ *E. coli* alanine racemase (unit defined in **S.1.2.6.2.**) to convert *L*-alanine to its *D*-stereoisomer which could be detected *via* the *D*-amino acid oxidase/horse radish peroxidase couple. Alternatively, a discontinuous method was developed where in a final volume of 196 µl, 50 mM *bis*-Tris propane pH 8.5, 20 mM $MgCl_2$, 0.13% (v/v) Triton X-100, 1.97 µM LpoB, 20 µM lipid II-Lys donor (C-terminal *L*-alanine or *D*-alanine), 20 µM MurNAc *meso*-DAP pentapeptide acceptor and 34.4 nM *E. coli* PBP 1B added from a freshly diluted stock in 25 mM Tris, 0.2% (v/v) Triton X-100, 10% (v/v) glycerol, pH 7.5 were incubated for 1 hour. The assay was terminated by addition 2.86 mM ampicillin and supplemented with 50 µl of 50 mM *bis*-Tris propane, pH 8.5, 14.45 $U.ml^{-1}$ *R. gracilis D*-amino acid oxidase, 5.71 $U.ml^{-1}$ horse radish peroxidase, 0.075 $U.ml^{-1}$ *E.*

coli alanine racemase, 0.1 mM pyridoxal phosphate, and 0.8 mM Amplex Red. The absorbance at 555 nm was followed until completion. Assay function was established by spiking assays that returned negative results with 5 μM *L*-alanine.

ASSOCIATED CONTENT

Material sources, protein analytical methods, purification methodologies for PBP1B, LpoB, DacB and alanine racemase from *E. coli* and *D*-amino acid oxidase from *R. gracilis*, mass spectrometric methods, preparation of transpeptidase donor and acceptor substrates, spectrophotometric and other enzyme assays and global non-linear analysis of kinetic data are recorded in Supplementary Data sections **S.1.1.**, **S.1.2.1.**, **S.1.2.2.**, **S.1.2.3.**, **S.1.2.4.**, **S.1.2.5.**, **S.1.2.6.**, **S.1.2.7.** and **S.1.2.8.** whilst Supplementary Results, References, Tables, F igures and their legends are recorded in Supplementary Data sections **S.2.** to **S.7.** inclusive. This material is available free of charge via the Internet at http://pubs.acs.org.

AUTHOR INFORMATION

Corresponding Authors[+]

A.J. Lloyd (Adrian.Lloyd@warwick.ac.uk) and C.G. Dowson (C.G.Dowson@warwick.ac.uk) School of Life Sciences, University of Warwick, Gibbet Hill Road, Coventry, CV2 2NX, UNITED KINGDOM.

Present Addresses

@S.C.: Microlease Ltd, Waverley Industrial Park, Hailsham Drive, Harrow, Middlesex, HA1 4TR, United Kingdom; †S.E.S.: Waters Corporation, Stamford Avenue, Altrincham Road, Wilmslow, SK9 4AX, United Kingdom; ‡G.P.: PhoreMost Ltd, Building 250, Babraham Research Campus, Cambridgeshire, CB22 3AT, United Kingdom; ¶N.F.G.: Department of Molecular Biology and Biotechnology, University of Sheffield, Western Bank, Sheffield S10 2TN, United Kingdom; §A.S.P.: Drug Discovery Unit, School of Life Sciences, University of Dundee, Dow Street Dundee DD1 5EH, United Kingdom; #D.R. Oxford Science Editing, John Eccles House, Oxford Science Park, Oxford, OX4 4GP, United Kingdom; [*]N.D.E. and *M.J.C.: School of Engineering, University of Warwick, Gibbet Hill Road, Coventry, CV4 7AL, United Kingdom.

Author Contributions

[$]A.C.C. and [$]A.J.L. contributed equally.

Notes

The authors have no competing interests to disclose.

ACKNOWLEDGMENT

The authors gratefully acknowledge the assistance provided by the Warwick/Waters Centre for BioMedical Mass Spectrometry and Proteomics and the media preparation facility in the School of Life Sciences of the University of Warwick. We wish to gratefully acknowledge the award to C.G.D. of grants from the BBSRC (BB/K017268/1), the MRC (G0701400, G1100127 and MR/N002679/1), the MRC Doctoral Training Programme at Warwick (MR/N014294/1) and to D.I.R. of BBSRC grant BB/N003241/1. We thank AstraZeneca Plc., for financial support and provision of facilities. We thank J. Deering and A. Dowson (Warwick) for assistance with the monofunctional transglycosylase assays and the Table of Contents image respectively.

REFERENCES

1. Vollmer, W.; Bertsche, U. Murein (peptidoglycan) structure, architecture and biosynthesis in *Escherichia coli*. *Biochim. Biophys. Acta* **2008**, 1778 (9), 1714-1734.
2. Fleming, A. On the antibacterial action of cultures of a Penicillium with special reference to their use in the isolation of *B. influenzae*. *Brit. J. Exp. Pathol.* **1929**, 10 (3), 226-236.
3. Macheboeuf, P.; Contreras-Martel, C.; Job, V.; Dideberg, O.; Dessen, A. Penicillin Binding Proteins: key players in bacterial cycle and drug resistance processes. *FEMS Microbiol. Rev.* **2008**, 30 (5), 673-691.
4. Sauvage, E.; Terrak, M. Glycosyl Transferases and Transpeptidases/Penicillin-Binding Proteins: Valuable Targets for New Antibacterials. *Antibiotics* **2016,** 5 (1), 12.
5. Hawkey, P.M. Multidrug-resistant Gram-negative bacteria: a product of globalisation. *J. Hosp. Infect.* **2015**, 89 (4)**,** 241-247.
6. Goffin, C.; Ghuysen, J. Biochemistry and Comparative Genomics of SxxK Superfamily Acyltransferases Offer a Clue to the Mycobacterial Paradox: Presence of Penicillin-Susceptible Target Proteins versus Lack of Efficiency of Penicillin as Therapeutic Agent. *Microbiol. Molec. Biol. Rev.* **2002**, 66 (4), 702-738.
7. Sauvage, E.; Kerff, F.; Terrak, M.; Ayala, J.A.; Charlier, P. The penicillin-binding proteins: structure and role in peptidoglycan biosynthesis. *FEMS Microbiol. Rev.* **2008**, 32 (5), 234-258.
8. Egan, A.J.F.; Biboy, J.; Van't Veer, I.; Breukink, E.; Vollmer, W. Activities and regulation of peptidoglycan synthases. *Phil. Trans. R. Soc. B.* **2015**, 370 (1679), 20150031.
9. Van Heijenoort, J. Lipid Intermediates in the Biosynthesis of Bacterial Peptidoglycan. *Microbiol. Molec. Biol. Rev.* **2007**, 71 (4), 620-635.
10. Josephine, H.R.; Charlier, P.; Davies, C.; Nicholas, R.A.; Pratt, R.F. Reactivity of Penicillin-Binding Proteins with Peptidoglycan-Mimetic β-Lactams: What's Wrong with These Enzymes? *Biochemistry* **2006**, 45 (51), 15873-15883.
11. Lloyd, A.J.; Gilbey, A.M.; Blewett, A.M.; De Pascale, G.; El Zoeiby, A.; Levesque, R.C.; Catherwood, A.C.; Tomasz, A.; Bugg, T.D.; Roper, D.I.; Dowson, C.G. Characterization of tRNA-dependent Peptide Bond Formation by MurM in the Synthesis of *Streptococcus pneumoniae* Peptidoglycan. *J. Biol. Chem.* **2008**, 283 (10), 6402-6417.
12. Clarke, T.B.; Kawai, F.; Park, S.Y.; Tame, J.R.; Dowson, C.G.; Roper, D.I. Mutational Analysis of the Substrate Specificity of *Escherichia coli* Penicillin Binding Protein 4. *Biochemistry* **2009**, 48 (12), 2675-2683.
13. Yousif, S.Y.; Broome-Smith, J.K.; Spratt, B.G. Lysis of *Escherichia coli* by β-Lactam Antibiotics: Deletion Analysis of the Role of Penicillin-binding Proteins 1A and 1B. *J. Gen. Microbiol.* **1985**, 131 (10), 2839-2845.

14. Suzuki, H.; Nishimura, Y.; Hirota, Y. On the process of cellular division in *Escherichia coli*: A series of mutants of *E.coli* altered in the penicillin-binding proteins. *Proc. Natl. Acad. Sci. U.S.A.* **1978**, 75 (2), 664-668.
15. Schiffer, G.; Höltje, J. Cloning and Characterization of PBP1C, a Third Member of the Multimodular Class A Penicillin-binding Proteins of *Escherichia coli*. *J. Biol. Chem.* **1999**, 274 (45), 32031-32039.
16. Paradis-Bleau, C.; Markovski, M.; Uehara, T.; Lupoli, T.J.; Walker, S.; Kahne, D.E.; Bernhardt, T.G. Lipoprotein Cofactors Located in the Outer Membrane Activate Bacterial Cell Wall Polymerases. *Cell* **2010**, 143 (7), 1110-1120.
17. Typas, A.; Banzhaf, M.; van den Berg van Saparoea, B.; Verheul, J.; Biboy, J.; Nichols, R.J.; Zietek, M.; Beilharz, K.; Kannenberg, K.; von Rechenberg, M.; Breukink, E.; den Blaauwen, T.; Gross, C.A.; Vollmer, W. Regulation of Peptidoglycan Synthesis by Outer-Membrane Proteins. *Cell* **2010**, 143 (7), 1097-1109.
18. Egan, A.J.F.; Jean, N.L.; Koumoutsi, A.; Bougault, C.M.; Biboy, J.; Sassine, J.; Solovyova, A.S.; Breukink, E.; Typas, A.; Vollmer, W.; Simorre, J.P. Outer-Membrane lipoprotein LpoB spans the periplasm to stimulate the peptidoglycan synthase PBP1B. *Proc. Natl. Acad. Sci. U.S.A.* **2014**, 111 (22), 8197-8202.
19. Mengin-Lecreulx, D.; Falla, T.; Blanot, D.; van Heijenoort, J.; Adams, D.J.; Chopra, I. Expression of the *Staphylococcus aureus* UDP-*N*-Acetylmuramoyl-L-Alanyl-D-Glutamate: |L-Lysine Ligase in *Escherichia coli* and Effects on Peptidoglycan Biosynthesis and Cell Growth. *J. Bacteriol.* **1999**, 181 (19), 5909-5914.
20. Lupoli, T.J.; Tsukamoto, H.; Doud, E.H.; Wang, T.S.; Walker, S.; Kahne, D. Transpeptidase-Mediated Incorporation of D-Amino Acids into Bacterial Peptidoglycan. *J. Am. Chem. Soc.* **2011**, 133 (28), 10748-10751.
21. Terrak, M.; Ghosh, T.K.; van Heijenoort, J.; Van Beeumen, J.; Lampilas, M.; Aszodi, J.; Ayala, J.A.; Ghuysen, J.M.; Nguyen-Distèche, M. The catalytic, glycosyl transferase and acyl transferase modules of the cell wall peptidoglycan-polymerizing penicillin-binding protein 1b of *Escherichia coli*. *Mol. Microbiol.* **1999**, 34 (2), 350-364.
22. Bertsche, U.; Breukink, E.; Kast, T.; Vollmer, W. In Vitro Murein (Peptidoglycan) Synthesis by Dimers of the Bifunctional Transglycosylase-Transpeptidase PBP1B from *Escherichia coli*. *J. Biol. Chem.* **2005**, 280 (45), 38096-38101.
23. Lupoli, T.J.; Lebar, M.D.; Markovski, M.; Bernhardt, T.; Kahne, D.; Walker, S. Lipoprotein Activators Stimulate *Escherichia coli* Penicillin-Binding Proteins by Different Mechanisms. *J. Am. Chem. Soc.* **2014**, 136 (1)**,** 52-55.
24. King, D.T.; Wasney, G.A.; Nosella, M.; Fong, A.; Strynadka, N.C.J. Structural Insights into Inhibition of *Escherichia coli* Penicillin-binding Protein 1B. *J. Biol. Chem.* **2017**, 292 (3), 979-993.
25. Hugonnet, J.; Mengin-Lecreulx, D.; Monton, A.; den Blaauwen, T.; Carbonnelle, E.; Veckerlé, C.; Brun, Y.V.; van Nieuwenhze, M.; Bouchier, C.; Tu, K.; Rice, L.B. Arthur, M. Factors essential for L,D-transpeptidase-mediated peptidoglycan cross-linking and β-lactam resistance in *Escherichia coli*. *eLife* **2016**, 5, e19469.
26. Schleifer, K.H.; Kandler, O. Peptidoglycan Types of Bacterial Cell Walls and their Taxonomic Implications. *Bacteriol. Rev.* **1972**, 36 (4), 407-477.
27. Mengin-Lecreulx, D.; Michaud, C.; Richaud, C.; Blanot, D.; Van Heijenoort, J. Incorporation of LL-Diaminopimelic Acid into Peptidoglycan of *Escherichia coli* Mutants Lacking Diaminopimelate Epimerase Encoded by *dapF*. *J. Bacteriol.* **1988**, 170 (5), 2031-2039.
28. Segel, I.H. Steady state kinetics of multi-reactant enzymes. Ch. 6. in: *Enzyme Kinetics: Behavior and Analysis of Rapid Equilibrium and Steady-State Enzyme Systems;* Wiley Classics Library Edn. John Wiley & Sons, N. Jersey 1975, pp. 273-345.
29. Kumar, P.; Kaushik, A.; Lloyd, E.P.; Li, S.G.; Mattoo, R.; Ammerman, N.C.; Bell, D.T.; Perryman, A.L.; Zandi, T.A.; Ekins, S.; Ginell, S.L.; Townsend, C.A.; Freundlich, J.S.; Lamichhane, G. Non-Classical transpeptidases yield insight into new antibacterials. *Nat. Chem. Biol.* **2017**, 13 (1)**,** 54-61.
30. Wickus, G.G.; Strominger, J.L. Penicillin-sensitive Transpeptidation during Peptidoglycan Biosynthesis in Cell-free Preparations from *Bacillus megaterium*: I. INCORPORATION OF FREE DIAMINOPIMELIC ACID INTO PEPTIDOGLYCAN. *J. Biol. Chem.* **1972**, 247 (17), 5297-5306.
31. Blumberg, P.M.; Strominger, J.L. Interaction of penicillin with the bacterial cell: penicillin-binding proteins and penicillin-sensitive enzymes. *Bacteriol. Rev.* **1974**, 38 (3), 291- 335.
32. Qiao, Y.; Srisuknimit, V.; Rubino, F.; Schaefer, K.; Ruiz, N.; Walker, S.; Kahne, D. Lipid II overproduction allows direct assay of transpeptidase inhibition by β-lactams. *Nat. Chem. Biol.* **2017**, 13 (7)**,** 793-798.
33. Adam, M.; Damblon, C.; Jamin, M.; Zorzi, W.; Dusart, V.; Galleni, M.; el Kharroubi, A.; Piras, G.; Spratt, B.G.; Keck, W. Acyltransferase activities of the high-molecular-mass essential penicillin-binding proteins. *Biochem. J.* **1991**, 279 (2), 601-604.
34. Van't Veer, I.L.; Leloup, N.O.; Egan, A.J.; Janssen, B.J.; Martin, N.I.; Vollmer. W.; Breukink, E. Site-Specific Immobilization of the Peptidoglycan Synthase PBP1B on a Surface Plasmon Resonance Chip Surface. *ChemBioChem* **2016**, 17 (23), 2250-2256.
35. Zapun, A.; Philippe, J.; Abrahams, K.A.; Signor, L.; Roper, D.I.; Breukink, E.; Vernet, T. In vitro Reconstitution of Peptidoglycan Assembly from the Gram-Positive Pathogen *Streptococcus pneumoniae*. *ACS Chem. Biol.* **2013**, 8 (12), 2688-2696.
36. Mishin, V.; Gray, J.P.; Heck, D.E.; Laskin, D.L., Laskin, J.D. Application of amplex red/horse radish peroxidase assay to measure hydrogen peroxide generation by recombinant microsomal enzymes. *Free Radic. Biol. Med.* **2010**, 48 (11), 1485-1491.
37. Sung, M.T.; Lai, Y.T.; Huang, C.Y.; Chou, L.Y.; Shih, H.W.; Cheng, W.C.; Wong, C.H.; Ma, C. Crystal structure of the membrane-bound bifunctional transglycosylase PBP1b from *Escherichia coli*. *Proc. Natl. Acad. Sci. U.S.A.* **2009,** 106 (22), 8824-8829.
38. Gray, A.N.; Egan, A.J.; Van't Veer, I.L.; Verheul, J.; Colavin, A.; Koumoutsi, A.; Biboy, J.; Altelaar, A.F.; Damen, M.J.; Huang, K.C.; Simorre, J.P.; Breukink, E.; den Blaauwen, T.; Typas, A.; Gross, C.A.; Vollmer W. Coordination of peptidoglycan synthesis and outer membrane constriction during *Escherichia coli* cell division. *eLife* **2015**, 4, e07118.
39. Ranjit, D.K.; Jorgenson, M.A.; Young, K.D.; PBP1B Glycosyltransferase and Transpeptidase Activities Play Different Essential Roles during the *De Novo* Regeneration of Rod Morphology in *Escherichia coli*. *J. Bacteriol.* **2017**, 199 (7), e00612-616.
40. Born, P.; Breukink, E.; Vollmer, W. *In Vitro* Synthesis of Cross-linked Murein and Its Attachment to Sacculi by PBP1A from *Escherichia coli*. *J. Biol. Chem.* **2006**, 281 (37), 26985-26993.
41. Kim, D.H.; Lees, W.J.; Kempsell, K.E.; Lane, W.S.; Duncan, K.; Walsh, C.T. Characterization of a Cys115 to Asp Substitution in the *Escherichia coli* Cell Wall Biosynthetic Enzyme UDP-GlcNAc Enolpyruvyl Transferase (MurA) That Confers Resistance to Inactivation by the Antibiotic Fosfomycin. *Biochemistry* **1996**, 35 (15), 4923-4928.
42. Dhalla, A.M.; Yanchunas, J. Jr.; Ho, H.T.; Falk, P.J.; Villafranca, J.J.; Robertson, J.G. Steady-State Kinetic Mechanism of *Escherichia coli* UDP-*N*-Acetylenolpyruvyl-glucosamine Reductase. *Biochemistry* **1995**, 34 (16), 5390-5402.
43. Patin, D.; Boniface, A.; Kovač, A.; Hervé, M.; Dementin, S.; Barreteau, H.; Mengin-Lecreulx, D.; Blanot D. Purification and biochemical characterization of Mur ligases from *Staphylococcus aureus*. *Biochimie*. **2010**, 92 (12), 1793-1800.
44. Liu, Y.; Rodrigues, J.P.; Bonvin, A.M.; Zaal, E.A.; Berkers, C.R.; Heger, M.; Gawarecka, E.; Swiezewska, K.; Breukink, E.; Egmond, M.R. New Insight into the Catalytic Mechanism of Bacterial MraY

from Enzyme Kinetics and Docking Studies. *J. Biol. Chem.* **2016,** 291 (29)**,** 15057-15063.
45. Auger, G.; van Heijenoort, J.; Mengin-Lecreulx, D; Blanot, D. A MurG assay which utilises a synthetic analogue of lipid I. *FEMS Micro. Lett.* **2003**, 219 (1), 115-119.
46. Glauner, B.; Höltje, J.; Shwarz, U. The Composition of the Murein of *Escherichia coli*. *J. Biol. Chem.* **1988**, 263 (21), 10088-10095.
47. Chen, Y.; Zhang, W.; Shi, Q.; Hesek, D.; Lee, M.; Mobashery, S.; Shoichet, B.K. Crystal Structures of Penicillin-Binding Protein 6 from *Escherichia coli*. *J. Am. Chem. Soc.* **2009**, 131 (40), 13345-13354.
48. Ruane, K.M.; Lloyd, A.J.; Fülöp, V.; Dowson, C.G.; Barreteau, H.; Boniface, A.; Dementin, S.; Blanot, D.; Mengin-Lecreulx, D.; Gobec, S.; Dessen, A.; Roper, D.I. Specificity Determinants for Lysine Incorporation in *Staphylococcus aureus* Peptidoglycan as Revealed by the Structure of a MurE Enzyme Ternary Complex. *J. Biol. Chem.* **2013**, 288 (46), 33439-33448.
49. Bennett, B.D.; Kimball, E.H.; Gao, M.; Osterhout, R.; Van Dien, S.J.; Rabinowitz, J.D. Absolute metabolite concentrations and implied enzyme active site occupancy in *Escherichia coli*. *Nat. Chem. Biol.* **2009**, 5 (8), 593-599.
50. Kumar, I.; Pratt, R.F. Transpeptidation Reactions of a Specific Substrate Catalysed by the *Streptomyces* R61 DD-Peptidase: The Structural Basis of Acyl Acceptor Specificity. *Biochemistry* **2005**, 44 (30), 9961-9970.
51. McDonough, M.A.; Anderson, J.W.; Silvaggi, N.R.; Pratt, R.F.; Knox, J.R.; Kelly, J.A. Structures of Two Kinetic Intermediates Reveal Species Specificity of Penicillin-binding Proteins. *J. Mol. Biol.* **2002**, 322 (1), 111-122.
52. Ito, E.; Strominger, J.L. Enzymatic Synthesis of the Peptide in Bacterial Uridine Nucleotides. II. Enzymatic synthesis and addition of D-alanyl-D-alanine. *J. Biol. Chem.* **1962**, 237 (8), 2696-2703.
53. Nieto, M.; Perkins, H.R.; Leyh-Bouille, M.; Frère, J.M.; Ghuysen, J.M. Peptide Inhibitors of *Streptomyces* DD-Carboxypeptidases. *Biochem. J.* **1973**, 131 (1)**,** 163-171.
54. Perkins, H.R.; Nieto, M. *Streptomyces* DD-Carboxypeptidases as Transpeptidases. *Biochem. J.* **1973**, 131 (4), 707-718.
55. Barreteau, H.; Kovac, A.; Boniface, A.; Sova, M.; Gobec, S.; Blanot, D. Cytoplasmic steps of peptidoglycan biosynthesis. *FEMS Microbiol. Rev.* **2008**, 32 (2), 168-207.
56. Ruiz, N. Lipid Flippases for Bacterial Peptidoglycan Biosynthesis. *Lipid Insights* **2015,** 8 (1), 21-31.
57. Van Heijenoort, Y.; Gómez, M.; Derrien, M.; Ayala, J.; Van Heijenoort, J. Membrane Intermediates in the Peptidoglycan Metabolism of *Escherichia coli*: Possible Roles of PBP 1b and PBP 3. *J. Bacteriol.* **1992**, 174 (11), 3549-3557.
58. Shi, Q.; Meroueh, S.O.; Fisher, J.F.; Mobashery, S. Investigation of the Mechanism of the Cell Wall DD-Carboxypeptidase Reaction of Penicillin-Binding Protein 5 of *Escherichia coli* by Quantum Mechanics/Molecular Mechanics Calculations. *J. Am. Chem. Soc.* **2008**, 130 (29), 9293-9303.
59. Frère, J.M.; Leyh-Bouille, M.; Ghuysen, J.M.; Perkins, H.R. Interaction between β-Lactam Antibiotics and Exocellular DD-Carboxypeptidase-Transpeptidase of *Streptomyces* R61. *Eur. J. Biochem.* **1974**, 50 (1), 203-214.
60. Miller, C.; Thomsen, L.E.; Gaggero, C.; Mosseri, R.; Ingmer, H.; Cohen, S.N. SOS Response Induction by β-Lactams and Bacterial Defense Against Antibiotic Lethality. *Science* **2004**, 305 (5690), 1629-1631.
61. Frère, J.M.; Ghuysen, J.M.; Perkins, H.; Nieto, M. Kinetics of Concomitant Transfer and Hydrolysis Reactions Catalysed by the Exocellular DD-Carboxypeptidase-Transpeptidase of *Streptomyces* R61. *Biochem. J.* **1973**, 135 (3), 483-492.
62. Jamin, M.; Wilkin, J.M.; Frère, J.M. A New Kinetic Mechanism for the Concomitant Hydrolysis and Transfer Reactions Catalysed by Bacterial-Peptidases. *Biochemistry* **1993**, 32 (28), 7278-7285.
63. Zhou, M.; Diwu, Z.; Panchuk-Voloshina, N.; Haugland, R.P. A Stable Nonfluorescent Derivative of Resorufin for the Fluorometric Determination of Trace Hydrogen Peroxide: Applications in Detecting the Activity of Phagocyte NADPH Oxidase and Other Oxidases. *Analyt. Biochem.* **1997**, 253 (2), 162–168.
64. Copeland, R.A. Appendix 5. In: Evaluation of Enzyme inhibitors in Drug Discovery: A Guide for Medicinal Chemists and Phamacologists. 2nd Edition, John Wiley and Sons Inc., New Jersey 2013, pp.493-495.